



POLITECNICO DI TORINO

DIPARTIMENTO DI ELETTRONICA E TELECOMUNICAZIONI
(DET)

Master's Degree in Biomedical Engineering

Measurement automation to control brain-machine interfaces

Supervisors

Prof. Valentina AGOSTINI

Dr. Ágoston Csaba HORVÁTH

Dr. Zoltán FEKETE

Candidate

Michele DETTO

TORINO, December 2020



PÁZMÁNY PÉTER KATOLIKUS EGYETEM



Abstract

The brain is one of the most temperature-sensitive organs in the human body, and this feature can be often linked to physiological phenomena and anomalies. Innovative state-of-the-art devices can investigate the neuronal response to temperature transients to assess, for instance, neurodegenerative diseases evolutions. For this purpose, implantable optical stimulation microdevices, or simply optrodes, have been designed by the Research Group of Implantable Microsystems, Pázmány Péter Catholic University, in collaboration with the Hungarian Academy of Sciences. The optrodes are multimodal devices; they simultaneously provide information on thermal and electrophysiological variations, as well as IR infrared light delivery into neural tissue, in a spatially controlled manner. In this master thesis project, optrodes have been adopted in order to implement a Matlab-based closed-loop control system. Moreover, a graphical user interface (GUI) has been developed to enable brain researchers to use the control system. Once the user has set up the necessary parameters, through the provided GUI, the user kickstarts the procedure. The control procedure begins with the 4-wire measurement of the optrode-integrated Pt filament sensor's resistance; this measurement is then converted into temperature values through the Callendar-Van Dusen relation. The temperature measurements are then used as control values for the control software, to decide whether IR irradiation by the optrode is required. Consequently, the IR irradiation causes thermal increase which continues to be monitored by the closed-loop system until any stop conditions are met. The light irradiation is performed through the communication between the software and a Source-measure Unit (SMU) which provides a DC supply current to an IR laser diode optically coupled to the optrode's Si waveguide, causing the IR light delivery from the microdevice tip. The achieved control system can adjust the DC supply current value according to the measured temperature in every loop cycle. In critical cases or in the presence of anomalies the system can: temporarily pause instruments intervention automatically (e.g. tissue overheating prevention), exit from control loop and end instruments communication automatically (e.g. maximum laser diode's working current exceeding) as well as through the user action. All the design choices for the software realization benefit both from the literature analysis, particularly the research concerning rats neocortex IR irradiation as well as instrument specification datasheet and manuals. The design process has been clearly outlined, from measurements accuracy calculations to IR diode's supply current values assessment, in relation to the optical power provided. Furthermore, parameters choices concerning the correct SMU communication, expressed in LUA programme language, have been justified. The control system

operation has been demonstrated by using tap water; thus, it aims to be a promising experimental tool to reveal thermal behaviour by way of self-adjusting control software.

Contents

Abstract	IV
List of Tables	VIII
List of Figures	IX
1 Introduction	1
2 Backgrounds	2
2.1 Closed-loop control systems	2
2.2 Temperature role and its control within the central nervous system.....	5
2.3 INS and INI techniques	9
3 Methods	11
3.1 IR Optrodes	11
3.2 Description of the used measurement methods.....	16
3.3 The chosen control system	20
4 Detailed introduction of the control system	24
4.1 The Graphical User Interface (GUI)	24
4.2 The start of the closed-loop control and the overall program	27
4.3 Source-measure Unit's parameters settings	32
4.4 The temperature measurement's approach	45
4.5 Exposure time's counting method	48
4.6 Temperature error calculation and the accuracy's role.....	51
4.7 The end of the closed-loop control.....	54
5 Validation	55
5.1 System behaviour in regular operation.....	55
5.2 Inappropriate set maximum exposure time demonstration	56

5.3	Maximum working diode current exceeding demonstration.....	57
5.4	Set maximum exposure time validation	58
5.5	Evaluation of the resistance batches acquisition duration.....	60
5.6	Recommended “Phase ON” values range for the user	61
5.7	Target temperature lower than room temperature test	65
5.8	IR illumination pause test.....	67
5.9	Live “Target Temperature” editing	67
5.10	Live supply current phase ON editing.....	69
6	Potential applications and benefits	70
7	Conclusions.....	72
8	Acknowledgement.....	76
9	References.....	78

List of Tables

Table 3.2.1 Optrodes' temperature sensor coefficients..... 19

Table 4.3.1 Most relevant parameters of the Thorlabs LPSC-1550-FG105LCA-SMA laser diode's datasheet..... 34

Table 4.3.2 Thorlabs LPSC-1550-FG105LCA-SMA laser diode's absolute maximum ratings. 34

Table 4.3.3 Slope efficiency's mean values of the three inspected optrodes. 37

Table 5.4.1 ΔT and accuracy values of the last five measured temperature values observed in figure 5.4.1..... 60

List of Figures

Figure 2.1.1 Closed-loop control's blocky graphic.	2
Figure 2.1.2 PID control's blocky graphic.	4
Figure 2.2.1 Dependence of brain structures on temperature.	6
Figure 2.2.2 Heat-gated TRPV1 ion channel.	7
Figure 2.2.3 Firing rate of hippocampal multiunit for various excitation powers.	8
Figure 3.1.1 The packaged IR optrode microdevice while facing 2 ml of tap water.	11
Figure 3.1.2 Multimodal optrode system concept.	12
Figure 3.1.3 Zoom of the optrode's top side final part (100 μm scale).	12
Figure 3.1.4 Schematic representation of the technology process flow of optrode fabrication.	13
Figure 3.1.5 Components of the packaged optrode.	14
Figure 3.1.6 The packaged optrode device.	15
Figure 3.2.1 Relative position of the optrode's tip and the IR detector's active surface.	16
Figure 3.2.2 Photo of the arrangement of absolute optical power measurement.	17
Figure 3.2.3 Photo of the measurement setup to characterize the waveguiding efficiency of fully packaged optrodes.	17
Figure 3.2.4 The 4-wire resistance measurement setup and the whole arrangement.	19
Figure 3.3.1 Experimental closeup that pictures the main elements interacting with the optrode. ..	21
Figure 3.3.2 The operational flow of the proposed closed-loop control in full operation.	23
Figure 4.1.1 The GUI before setting all input parameters.	24
Figure 4.1.2 The optrodes' popup menu.	25
Figure 4.1.3 The user-editable Target Temperature box.	25
Figure 4.1.4 The user-editable maximum exposure time box.	25
Figure 4.1.5 The user-editable phase "ON" of the diode's supply current box.	26
Figure 4.1.6 Updated boxes of measured temperature and supply current value during the system operation.	26
Figure 4.2.1 The overall software flowchart.	31
Figure 4.3.1 Infrared irradiation of rat's cortical neurons at 1600 μm of depth.	33

Figure 4.3.2 A characteristic change in optical power vs driving current of laser diodes, for three different probes' features.	36
Figure 4.3.3 "Target not reached" branch.	39
Figure 4.3.4 Example of trigger event useful to let Timer #1 start counting its delay.	40
Figure 4.3.5 The remote trigger model.	42
Figure 4.3.6 Flowchart of the SMU's current sweep branch programming.	44
Figure 4.4.1 Flowchart of the temperature measurement phase.	46
Figure 4.5.1 "Target reached" branch.	50
Figure 5.1.1 Control system's GUI in regular operation conditions.	56
Figure 5.2.1 Incorrect "Time max" value demonstration.	57
Figure 5.3.1 Maximum working diode current exceeding.	58
Figure 5.4.1 Maximum exposure time validation.	59
Figure 5.5.1 Duration of the last batch's measurement/acquisition on five algorithm's launch trials.	61
Figure 5.6.1 "Phase ON" = 2 s trial.	62
Figure 5.6.2 "Phase ON" = 5 s trial.	63
Figure 5.6.3 "Phase ON" = 15 s trial.	64
Figure 5.6.4 "Phase ON" = 60 s trial.	65
Figure 5.7.1 Target Temperature lower than room temperature test.	66
Figure 5.8.1 "IR Pause Illumination" button use.	67
Figure 5.9.1 "Target Temperature" value live editing test.	68
Figure 5.10.1 "Phase ON" value live editing test.	69

1 Introduction

Nowadays, cellular response mapping, in the living brain, to temperature changes, is an essential object of research. So far, state of the art tells us that steps toward a realization of devices able to modulate temperature and to record stimulated area's features (such as precisely, the temperature itself), have been limited.

The Research Group of Implantable Microsystems, Pázmány Péter Catholic University, in collaboration with the Hungarian Academy of Sciences, has designed and characterized implantable optical stimulation microdevices (or briefly optrodes). Devices under investigation can deliver infrared light into the neural tissue in a spatially controlled manner. At the same time, they provide information on thermal and electrophysiological changes in the vicinity of the stimulated region (so integrating monolithically into a single device optical, thermal, and electrophysiological functions).

This thesis project aims to create a Matlab-based control system, used by brain researchers to realize neural stimulation by using infrared irradiation through optical actuators, and based on recorded data of the integrated sensors, the stimulating parameters during in vitro or in vivo experiments can be adjusted and controlled.

2 Backgrounds

2.1 Closed-loop control systems

At the basis of the system's realization capable of increasing the brain tissue temperature in a "controlled" and local manner, above all, there is the "closed-loop control" (CLC) concept.

What is it, then?

The closed-loop control (also called feedback control), despite the open-loop control, is a control mechanism in which the "current result", that is the every loop cycle's outcome, is continuously compared to the "reference result", as schematically explained in figure 2.1.1. In response to this comparison, specific process parameters are modified and adjusted in order to minimize more and more the difference between the results, by forcing the obtained response to follow the reference one[1]. A prevailing aspect which belongs to this control's type consists of the capability to automatically compensate every form of internal or external disturbance, due to the mechanism itself's kind.

Even though, in general, CLC is a more complex and expensive mechanism, it is increasingly used in the continuous processes' field, the ones such that analogic inputs and (or) outputs are used (by using appropriate instrumentation and devices).

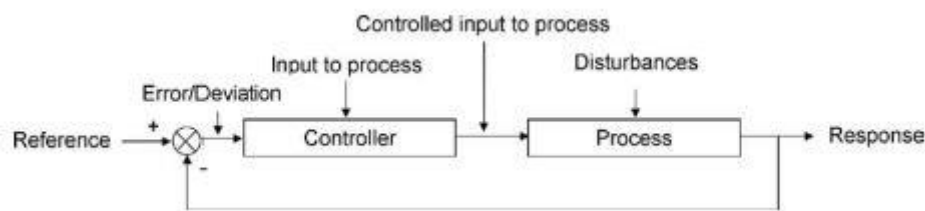


Figure 2.1.1 Closed-loop control's blocky graphic.

In this case, the CLC application in this type of processes arises from the need to continuously "trace" the output of the process (what was previously called "result"), compare it to the reference value and adjust the input parameters of the process to (ideally) cancel the error between the two values. It is implied that the instrumentation's data acquisition activity is also a continuous operation.

A practical example that brings us closer to everyday life can be the water heater's one, in which the "controller" is the variable which regulates the voltage source: the temperature is continuously measured and compared to the desired value. Consequently, water heating power will be proportional to the deviation between the two values.

If instead, we cite the "Deep Brain Stimulation" (DBS) technique, we would have made an example of CLC much closer to the world of Neuroengineering. Indeed, this technique is used to minimize the motor symptoms of a subject with Parkinson's disease, during which the stimulation parameters ("controllers") are continuously and automatically adjusted thanks to electrical signals feedback (Local Field Potential) taken from the same electrode implanted to perform the stimulation[2].

The error minimization in a control mechanism based on feedback, in particular, the role of "process controller", can find as a useful example among the options present at the current state of the art, the PID mode. The three letters of this acronym indicate the three methodologies used to determine the nature of the "output controller" of the mechanism. The three modes are commonly used together or, sometimes, only a combination of them is used: P = "proportional", I = "integral", D = "derivative"[3].

Wanting to analyze this type of closed-loop control briefly, we choose to describe the three functions taken into consideration one at a time.

The proportional action (P), alone, is precisely such because it is proportional to the error between the measured value and the reference value which, from now on, will be called "target" value. Given K_C as a constant of proportionality, the relationship that governs the action will be:

$$m = K_C \cdot e + b$$

where is it:

- m = output controller
- K_C = controller gain
- e = error
- b = external perturbation factor

The most evident limits, if only proportional action is used, are the failure to memorize the history of the measurement of the value concerned, nor of its frequency of variation.

The integral action (I) is proportional to the time integral of the error, multiplied by a constant; by adding the integral action to the previously mentioned proportional one, we obtain the relation:

$$m = K_C \cdot \left(e + \frac{1}{T_I} \int e dt \right)$$

where is it:

- T_I = integration time

In doing so, the output will keep the memory of the previous values assumed by the error.

Derivative action (D) primarily exists to improve controller performances. It is proportional to measurement's frequency of variation; ultimately, is achieved:

$$m = K_C \cdot \left(e + \frac{1}{T_I} \int e dt + T_D \frac{de}{dt} \right)$$

where is it:

- T_D = derivation time.

A PID-type output controller, therefore, contains these three actions, briefly described by the previous mathematical relationship and also summarized by the following figure 2.1.2:

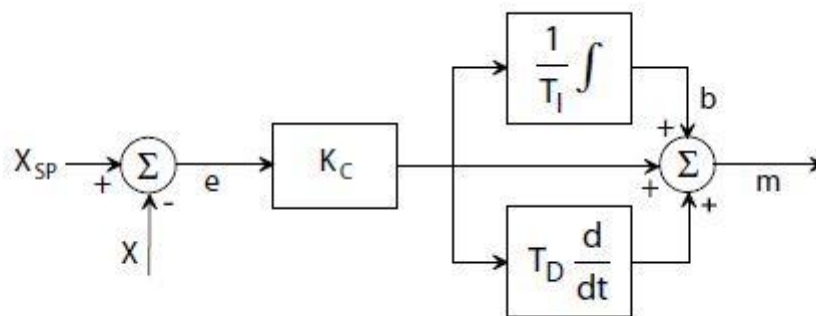


Figure 2.1.2 PID control's blocky graphic. The " X_{SP} " value (SP = "set point") is the target value, whereas " X " is the measured value.

This small digression can be concluded by citing a case in which Neuroengineering can use PID control. Returning to the previously mentioned DBS technique, the PID system is applied in order to modulate the amplitude of the electrical stimulation. Coming back to the equation which regulates the output controller ("m"), error "e" will be, in this case, the difference between the signal representing the oscillations in the beta band[4] and the set target value. The stimulation parameter useful for performing DBS, appropriately corrected through the PID system and essential to minimize motor discomfort in Parkinsonian subjects, will therefore be a function of "m".

Going back to the purpose of this thesis which, as anticipated, is to implement a closed-loop control mechanism, the temperature will be the variable to be iteratively measured and compared to a target value. Temperature is appropriately measured at the level of the brain area that circumscribes the stimulation site of the implanted optrode; the resulting controller output will have its primary purpose in the infrared light stimulation (at adjustable power), emitted by the optrode's tip. Reaching the maximum exposure time at the temperature pre-established by the user will be the sufficient and necessary condition to be able, if temperature greater than a threshold, to exit the implemented CLC system, a useful aspect also for any overheating of the affected tissues.

We now proceed to investigate, briefly, why temperature (and its control) is such an essential factor in the dynamics of the nervous system.

2.2 Temperature role and its control within the central nervous system

The brain is one of the most temperature-sensitive organs. Under a morphological point of view, looking at the figure 2.2.1 dependence of brain structures on temperature can be seen.

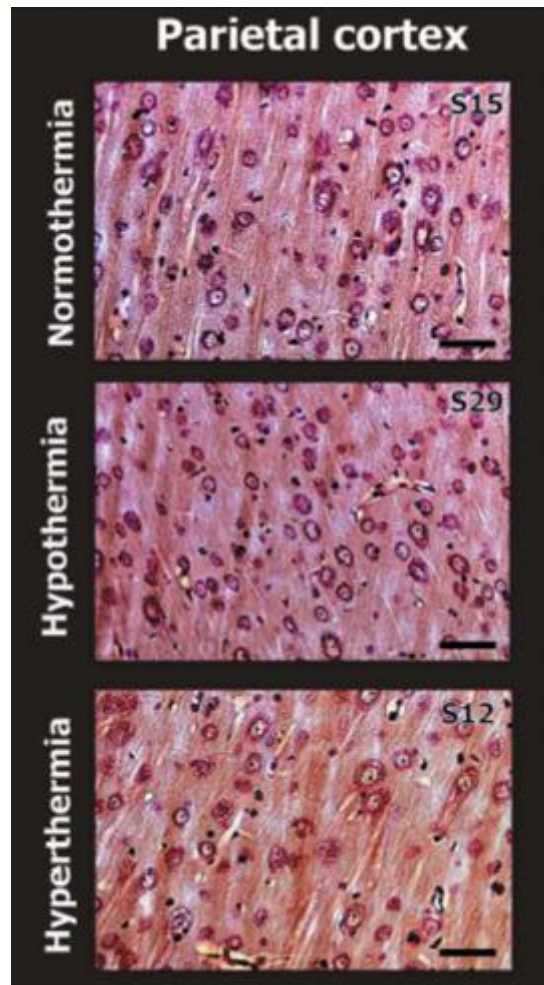


Figure 2.2.1 Dependence of brain structures on temperature[5].

Indeed, three sections of the rats' parietal cortex, stained with the Nissl method, respectively at 36.05 °C, 32.30 °C and 40.80 °C have been pictured. In conditions of hyperthermia, an enlargement of the soma and axons is noted, compared to a condition of normothermia.

Under normal physiological conditions, brain temperature changes can fluctuate between 2 and 4 °C[5], without this phenomenon being related to pathological phenomena. The thermal response from the neuronal populations plays an essential role in the study of neurodegenerative diseases (the presence of pathological hyperthermias, linked to low metabolic heat dissipation, in cases of ischemia, epilepsy and traumatic brain injuries has been discovered)[6].

Recent studies have shown that it is evident that temperature (and its impact) influences everyday neurophysiological phenomena.

Among these, there is cellular metabolism[6], where the percentage of dissipated heat would increase with the collaboration of the energy produced by the oxidative metabolism (although the subject may be in a state of rest). Something similar can be, for example, the metabolism phenomenon at the level of the BBB (Blood Brain Barrier), which in response to a specific thermal impact, sees its permeability increase[6].

First, progressive thermal injuries to metabolically active brain cells and BBB begin to manifest at temperatures between 39 and 40 °C[7].

Temperature is a relevant factor in intercellular communication: synaptic transmission is sensitive to heat and therefore modulated by temperature[8], due to the existence of thermally active receptors under absolutely physiological conditions, which see their channels' conductance increase (non-selective heat-gated ion channels, permeable to Na^+ , K^+ and Ca^{2+} ions[9], belonging to the family of TRP channels and present in a subset of primary afferent neurons[10], and more generally in the central and peripheral nervous system). A comprehensive graphical model of this sort of channel can be appreciated in figure 2.2.2: the TRPV1 channel has an activation threshold above 43 °C[11]. This sort of optimization of synaptic activity leads, like a domino effect, to an alteration of other fundamental cellular properties such as resting potential and action potential, hence their excitability.

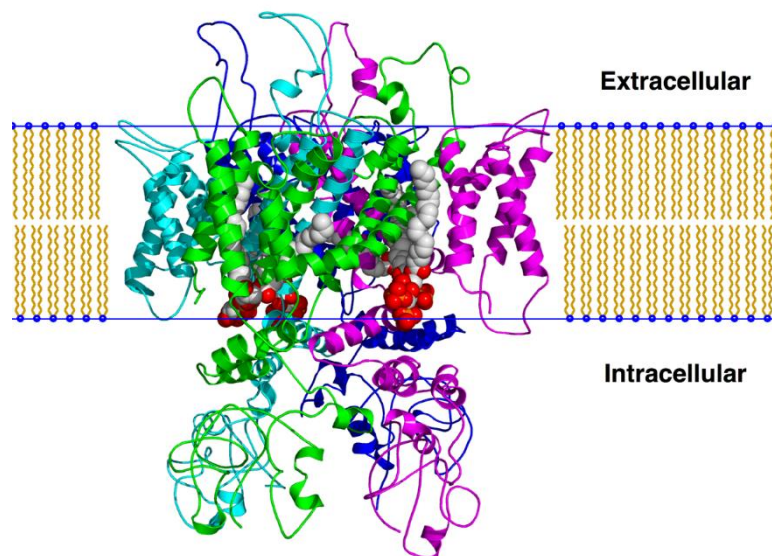


Figure 2.2.2 Heat-gated TRPV1 ion channel.

Horváth et al. also demonstrated the relationship between heating and neuronal electrical activity[6], as it can be noticed by observing figure 2.2.3.

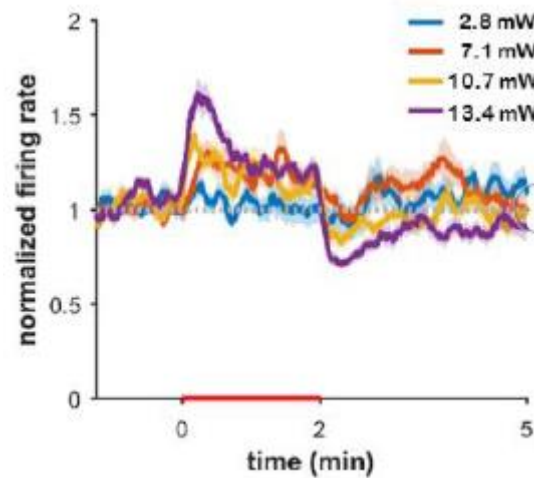


Figure 2.2.3 Firing rate of hippocampal multiunit for various excitation powers[6].

Considering the example pictured above, the firing rate of hippocampal multiunit for various excitation powers can be observed. Heating action, indicated by the red line on the time axis and caused by the IR light, was emitted from the tip of an optrode implanted in the brain of a Wistar rat during an in vivo experiment.

However, it should be noted that reaching temperatures between 42 and 43 °C leads on average to a severe risk of cessation of spontaneous neural activity[7].

Finding a way to stimulate the brain tissue locally, therefore in a spatially and energetically controlled modality, is essential for obtaining responses of the neuronal population in a local form, always however using energy sources that respect the set safety limits. In this way, real neuromodulation is obtained: this technique could allow us, for example, to obtain the activation of the visual cortex "simply" by using a controlled source of infrared stimulation.

At the same time, brain thermorecording, that is among the main actors of this study, according to the available literature, has never been an object of particular interest at the research level, perhaps because of the difficulties that have always been encountered in relating the temperature to the different forms and types through which neural activity occurs[5].

It must be emphasized, therefore, that the road that leads to an in-depth knowledge of the spatio-temporal distribution of the brain temperature and the role of this phenomenon in mechanisms such as cerebral homeostasis is still long.

2.3 INS and INI techniques

What are, according to the literature currently available, some of the most used techniques of brain tissue irradiation in the case in which the source of irradiation was light in the infrared spectrum and not there was a need, as happens in optogenetic techniques, for any viral modification?

Infrared Neural Stimulation (INS) and Infrared Neural Inhibition (INI) are two variants of the Infrared Neuromodulation (INM) photobiomodulating technique[12]. Neuromodulation generally intervenes in physiological processes of neural ensembles by using -in this case- optical means. The most commonly known disorders where neuromodulation can be used are Alzheimer's, Parkinson's disease and depression. In contrast with other techniques (such as electrical stimulation) irradiation is exploited avoiding any spreading phenomena. Furthermore, since the light source is delivered in a controlled manner, this sort of modulation can be repeatedly applied without any tissue damages. Lastly, such techniques can be used in conjunction with magnetic fields and so in magnetic resonance imaging applications, as well as with electrophysiology methods.

It should be noted that those INM techniques, beyond the primary effect concerning IR light delivery in a locally and controlled manner (so at small cellular ensembles level), even provide the secondary effect of CNS' network activity affection. For instance, it has been proven that transcranial near-infrared stimulation ($\lambda = 808$ nm) improves functional connectivity in chronic TBI (Traumatic Brain Injury) patients[13] and dementia patients[14].

INS uses pulsed infrared light (λ wavelength between 1400 and 2100 nm) to generate controlled thermal gradients (spatial dT/dx or temporal dT/dt) in neuronal cells in order, precisely, to stimulate them (thus triggering action potentials). It has been demonstrated that INS similarly acts on various cellular types, ranging from peripheral nerves[15] to sensory ganglion[16], as long as cardiac cells[17]. Liu et al.[18] demonstrated in 2014 that thermal shocks (500 °C/s for 500 μ s) even cause an excitatory currents asymmetry such that to induce depolarization phenomena at the cellular membrane level. It has also been hypothesized that nanopores creation through the plasma membrane, besides membrane thickness, can contribute to INS (and so temperature gradients) cellular

response[19]. Such nanopores creation, mainly due to intramembrane's phospholipids destabilization, allows Ca^{2+} extracellular ions into the cytoplasm, it is therefore the primary action potential firing cause in this case.

As described in the previous paragraph, an increase in action potentials firing is mainly due to an increase in synaptic transmission capacity. An uneven increase, on the other hand, of the gating mechanism (as described by the Hodgkin-Huxley theory[6]) at the level of temperature-dependent channels can lead the neuron to the opposite situation, that is to inhibition (action potential propagation blocking). This phenomenon, caused by an application of the infrared source, does not occur according to a space-time gradient but in a manner proportional to the basal temperature assumed by the district concerned. This technique, which precisely is the INI technique, on average employs lower optical powers of exposure (even below 14 mW[6]) and a continuous or pulsed light source. The underlying mechanism consists of potassium ion channels activation alongside the sodium channels inactivation, with a net increase of hyperpolarizing currents despite the depolarizing ones[20].

However, they must be mentioned the following points, as Horváth et al. have stated in recent studies:

- 1) there are neurons, such as those belonging to the intracortical and hippocampal areas, which can be both inhibited and stimulated using small space-time gradients at energies in the range of mW[6];
- 2) neuronal response to IR light can be cortex superficial layers-dependent. INS must be an operation, as far as possible, controlled and targeted, in order to avoid unexpected inhibitory responses. A relevant example may be the accidental irradiation of inhibitory interneurons of cortical layers I and II, during an INS session at layer V of the cerebral cortex.[6];
- 3) potential therapeutic capabilities have so far been found more with deep neural tissue stimulations rather than with superficial ones[21].

3 Methods

3.1 IR Optrodes

The device proposed to tackle this study is an innovative optrode developed by the Research Group of Implantable Microsystems, Pázmány Péter Catholic University.

The innovative turning point of this neural probe, designed to be implanted in deep brain tissue (in figure 3.1.1 it can be noticed a test simulation concerning the packaged microdevice inserted in 2 ml of tap water, as a similar water-content target to illuminate), is its "multimodal" nature[21].

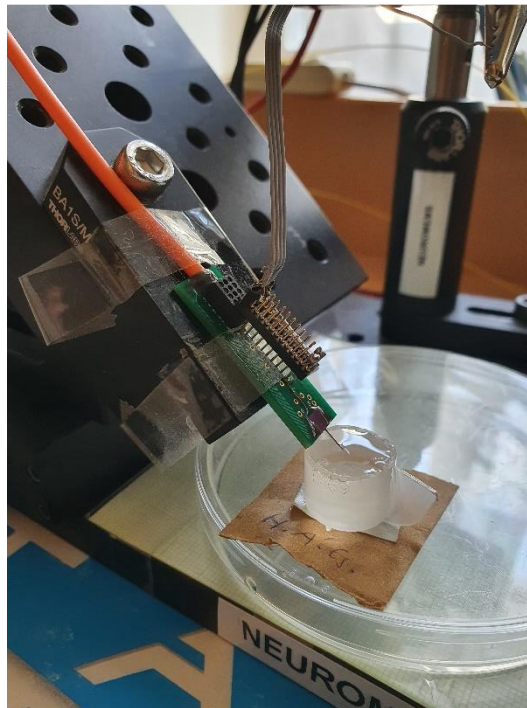


Figure 3.1.1 The packaged IR optrode microdevice while facing 2 ml of tap water.

Optical, thermal and electrophysiological functions have been integrated on the same device, as this optrode is capable, respectively, of spatially-controlled infrared light delivery, carrying out local temperature measurements and recording neural activity.

On this probe (5 mm long, 150 μm wide and 190 μm thick) there are four platinum recording sites along the probe shaft (at the tip of the optrode), with an intersite distance of 100 μm and each with a surface of 900 μm^2 , used for the electrical recording. These probe's features are graphically

represented in figure 3.1.3. A platinum filament, enclosed between a top and bottom thin films and located near the final part of the probe shaft's tip, is used as a temperature sensor (4 μm wide and 270 nm thick). As anticipated, the infrared light comes out of the optrode tip, how understandable from red arrows in figure 3.1.2.

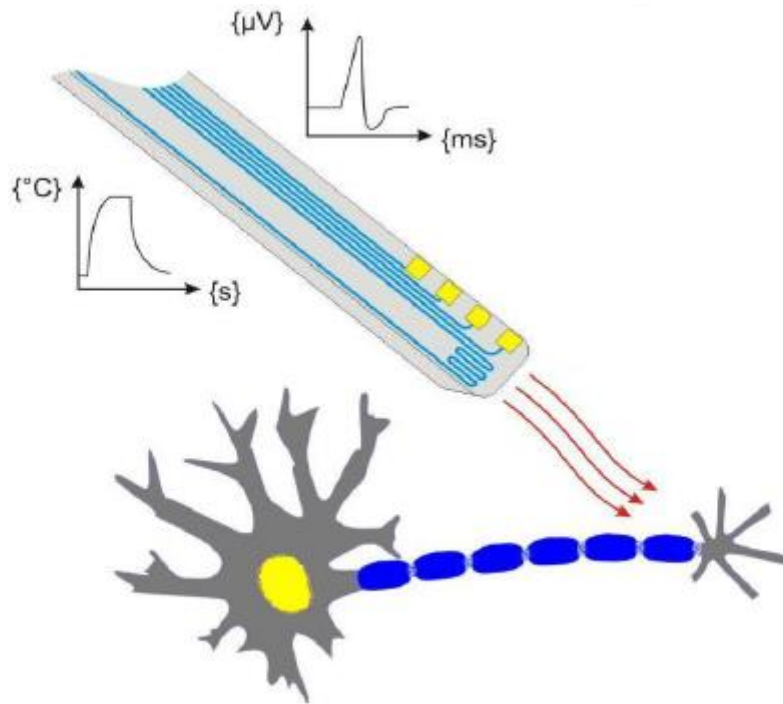


Figure 3.1.2 Multimodal optrode system concept.

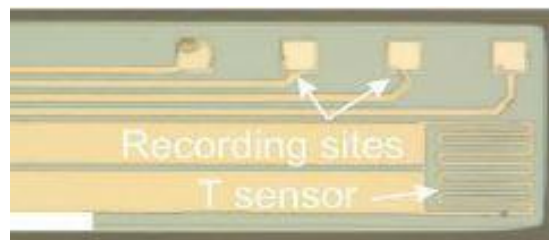


Figure 3.1.3 Zoom of the optrode's top side final part (100 μm scale).

The fabrication of this neural probe, as well as the integration of the three functionalities on a single platform, were obtained using silicon MEMS technology. The wafer, which begins as a monocrystalline silicon substrate (100), 200 μm thick, is first polished on both sides, in order to maximize the efficiency of the integrated Si waveguide and at the same time guarantee the wafer surface smoothness: it is emphasized a completely new peculiarity in the overall view of silicon substrates, which pass from a role purely assigned to mechanical stability, to having, thanks to

appropriate wet chemical etching interventions, to waveguiding capabilities. The roughness level on the shaft's surface allows avoiding significant losses of IR light at the sidewalls level, during its propagation in the integrated optical waveguide. In this way, the IR rays internal reflection inside the probe shaft is facilitated: sidewalls are thus rendered optically smooth.

The necessary manufacturing steps are described in the following figure 3.1.4:

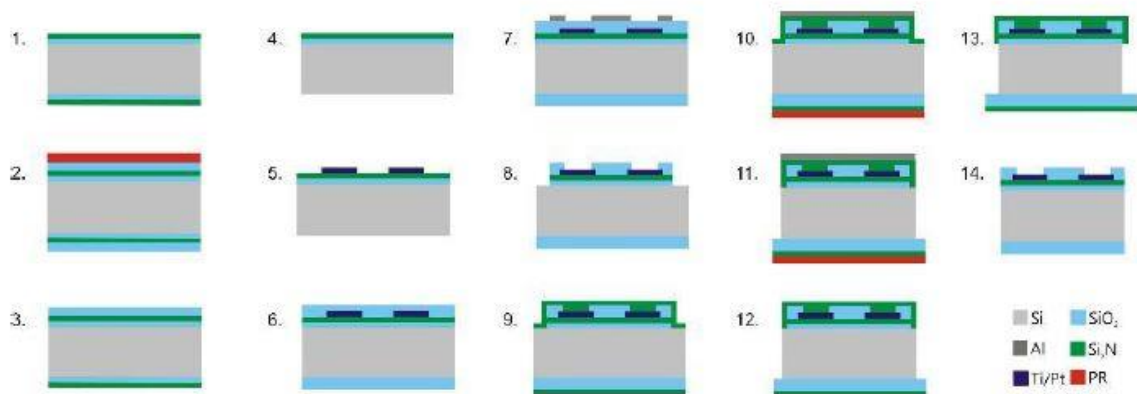


Figure 3.1.4 Schematic representation of the technology process flow of optrode fabrication. (1) SiO₂ and SiN deposition, (2) LTO (Low-Temperature Oxide) deposition and front-side photoresist (PR) protection, (3) HF (Hydrofluoric) etch and PR removal, (4) Backside nitride and oxide removal, (5) Ti/Pt deposition and lift-off, (6) LTO deposition, (7) Deposition, photolithography and etching of Al mask for DRIE (Deep Reactive Ion Etching), (8) Dielectric stack removal in DRIE and Al removal in the wet etchant, (9) SiN_x deposition, (10) Deposition, photolithography and etching of Al mask for DRIE with backside PR protective layer, (11) Deep silicon etching in DRIE, (12) Removal of Al mask and protective PR layer, (13) Wet chemical polishing, (14) HF etch and SiN removal in phosphoric acid[21].

Each of these steps is now linked to its purpose:

- step 1: recording sites areas isolation from the Si bulk;
- steps 2-4: SiN_x and SiO₂ removal from the wafer backside;
- step 5: recording sites, temperature monitoring filament and conductor paths patterns definition;
- step 6: top passivation layer to minimize corrosion phenomena;
- step 7: contact and bonding sites definition;
- step 8: SiO₂ / SiN₂ / SiO₂ dielectric stack removal;
- step 9: wet chemical polishing's masking layer definition;
- steps 10: backside protective photoresist layer definition;
- step 11: needle-like contour shaping, forming individual chips from the Si wafer
- step 12: masking layer removal;
- step 13: probe sidewalls planarization;

- step 14: top and bottom protective layers removal, window opening above recording sites and bonding pads.

After the microfabrication phase, the chip is packaged in order to couple it to its optical functionalities (i.e. its connection to the external light source) and insert the amplifiers for electrical recording and temperature measurements (see the drawing example in figure 3.1.5). A multimode optical fibre, whose core has a diameter of 105 μm , is mounted with an SMA connector and coupled to the optrode chip with the embedded fibre guide etched inside the chip's backbone. The chip is mounted on a Printed Board Circuit (wire bonding between the chip backbone's pads and the PCB's pads), which in turn is mounted on a PreciDip connector (Preci-dip SA, Switzerland) in order to provide the electrical connections and external amplifiers useful during in vivo testing. The packaging outcome can be seen in figure 3.1.6.

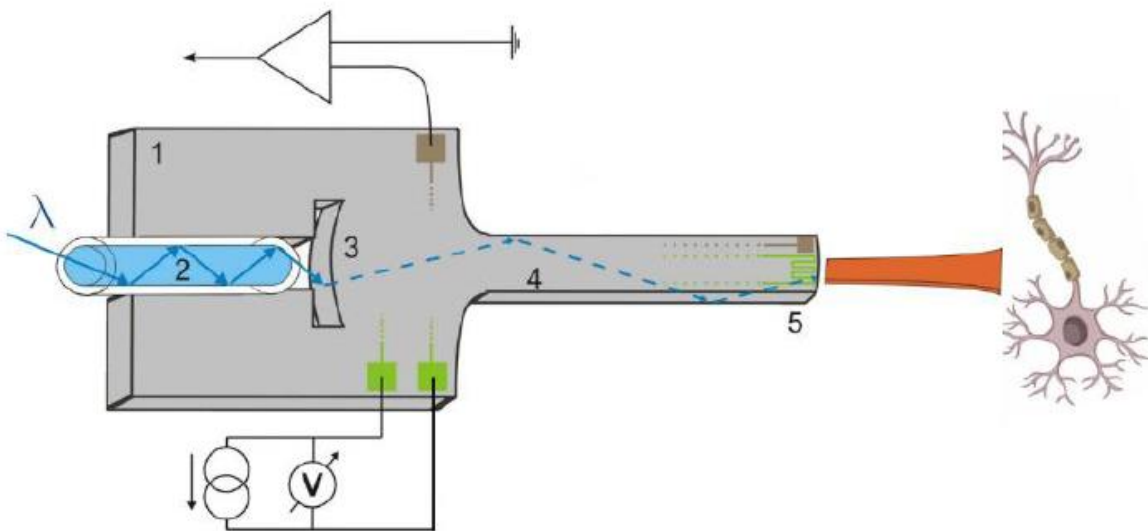


Figure 3.1.5 Components of the packaged optrode. (1) Si substrate, (2) Multimode optical fibre, (3) Coupling lens to allow the multimode fibre-embedded Si waveguide pairing, (4) Multifunctional probe shaft, (5) Probe tip.

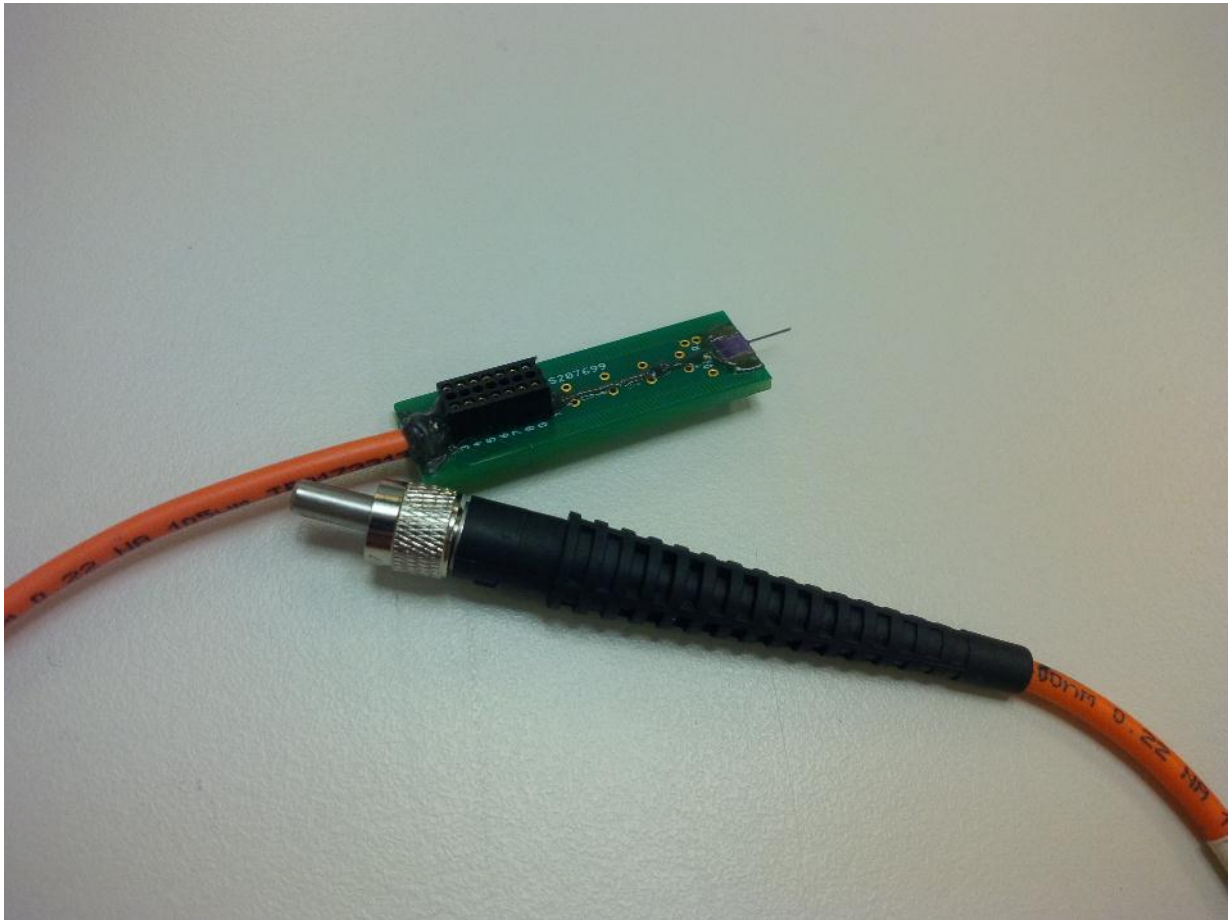


Figure 3.1.6 The packaged optrode device.

What about possible application perspectives? Abaya et al. suggested, regarding the local delivery of infrared light, a Utah-type array[22], although the choice made in the current project to use a Michigan-type configuration proved to be better, both in terms of depth of stimulation and reduction of passive optical elements to be applied to the probe (remember again that the waveguide is embedded). However, other variants could prove to be feasible, such as "multi-shaft" stimulation or exploiting the scalability of recording sites or shafts (and therefore of the waveguide) to suit their own experimental needs better. However, the substance does not change: the optrodes will allow to obtain and monitor, both from a thermal and electrical point of view, the activation of specific brain regions.

3.2 Description of the used measurement methods

Before the closed-loop system's development, it has been necessary to measure specific parameters for selecting out the useless optrodes which would not then have been implanted because of their too weak IR heating performance. In order to do this, specific tools and methodologies have been used.

The first to be mentioned is the determination of the absolute optical power exiting the probe tip. First of all, it should be noted that the external light source, suitably coupled to the multimodal fibre-probe system, is a Thorlabs LPSC-1550-FG105LCA infrared LASER diode (Thorlabs, Inc. USA) suitably driven (as will be described later) by an appropriate driving current (centre IR light wavelength $\lambda = 1550$ nm). The final output of this "chain" is precisely the IR light that comes out of the optrode tip: the measurement of its optical power is performed utilizing a Germanium IR sensor (OP-2 IR, Coherent Inc., CA, USA) connected to a laser power meter (FieldMaxII-TOP, Coherent Inc., CA, USA). During this measurement, the optrode is fixed on a mobile platform that moves along 1D and places in front of the power laser meter. In particular, the tip of the optrode is placed at $100\ \mu\text{m}$ from the active surface of the IR sensor, as exemplified in figure 3.2.1 and qualitatively pictured in figure 3.2.2.

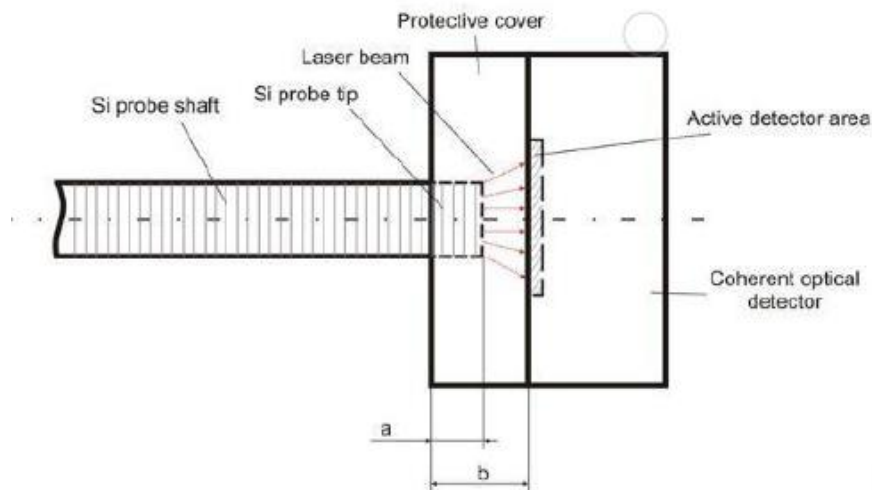


Figure 3.2.1 Relative position of the optrode's tip and the IR detector's active surface ($a = 7$ mm, $b = 7.1$ mm).

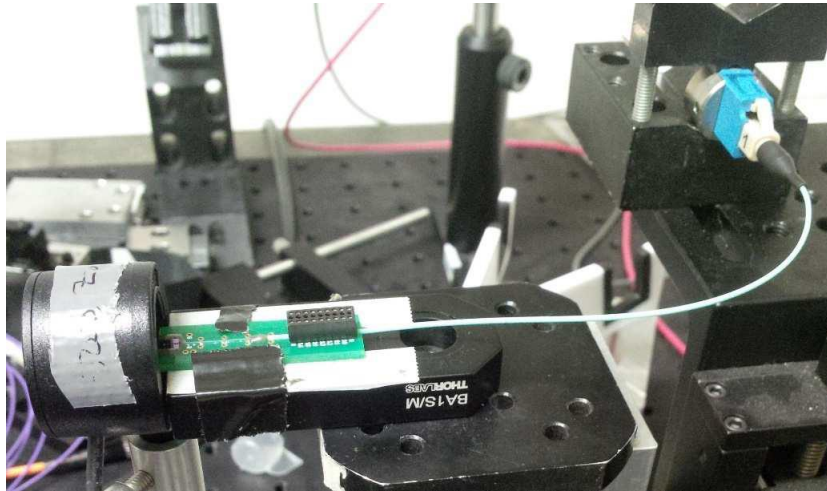


Figure 3.2.2 Photo of the arrangement of absolute optical power measurement[23].

The setup represented in figure 3.2.3 shows that another essential optical feature must be brought to attention to be measured and analyzed. In this case, Waveguiding Efficiency (WGE) is measured with the aim to evaluate the probe's shaft as passive infrared waveguide[21].



Figure 3.2.3 Photo of the measurement setup to characterize the waveguiding efficiency of fully packaged optrodes. Collimated IR light ($\lambda = 1310$ nm) emitted from a laser diode (1) is focused on the front facet of the multimode fibre (2), which is part of the optrode device. The PCB (3) of the optrode under test is fastened on a 3D translation stage. Imaging (4) the plane of the optrode end facet is made by a microscope objective (50 \times , NA = 0.8). All measured data are registered by a CMOS beam profiler (5). Scale bar shows 2 cm.

The overall efficiency is given by:

$$\eta = \frac{(P_{optrode})}{(P_{fibre})} \cdot 100 [\%]$$

which is the ratio between the beam power exiting from the fibre guide and the power exiting the fully assembled optrode's tip, expressed as a percentage.

Fully packaged optrode devices were placed in the light path between the IR source and the measuring instrument (CMOS beam profiler) to investigate the overall device WGE[21]. Before placing the assembled optrode in the light path, an optical fibre is applied to measure the fibre intensity, set as reference value.

The role of the integrated platinum filament used for temperature measurement is also central.

It falls into one of the leading temperature sensors' categories, the RTDs ("Resistance Temperature Detectors"). It is, therefore, a resistive sensor, characterized by a Resistive Temperature Coefficient (TCR) and whose resistance value (in Ω) increases with increasing temperature. So it is possible to get the relative temperature by employing resistance measurements. This value will ideally correspond to the exact temperature to which the platinum filament is exposed, at the time of measurement. The Callendar-Van Dusen equation regulates the conversion from the measured resistance value into the corresponding temperature value (in $^{\circ}\text{C}$):

$$R_T = R_0(1 + \alpha T)$$

with:

- R_T = resistance value measured at temperature T [Ω];
- R_0 = resistance value assumed at 0 $^{\circ}\text{C}$ [Ω];
- T = temperature [$^{\circ}\text{C}$];
- α = TCR [$1 / ^{\circ}\text{C}$].

R_0 and α are therefore tabulated values that characterize an individual Pt resistor and, in this case, a certain optrode. In this thesis, three different optrodes have been taken into account. The reason why the developed software will have available (as will also be explained later) three possible R_0 / α values pairs, to be able to work individually with any of the three possible optrodes objects of this study and then control the optrode correctly. These constant values were obtained through calibration procedures (carried out before this thesis work) during which the three optrode microdevices were immersed in a liquid medium of physiological saline, at a depth of 2 mm. Therefore, by modifying, at the same temperature of the medium, the depth of the optrodes in the medium itself, the measured resistance value should be different. However, with the same optrode, the calibration curves' slope as varying the depth in the medium turned out to be very similar to each other, i.e. a variation in

temperature always corresponds to a similar variation in terms of resistance. Said that, since there are no significant differences, these pairs of R_0 / α values are considered definitive and characterizing each of these three optrodes (which will be called OT1, OT2, OT3). The values are shown in table 3.2.1 below:

	R_0 [Ω]	TCR [$1 / ^\circ\text{C}$]
OT1	358.5574	$2.6505 \cdot 10^{-3}$
OT2	347.2003	$2.5387 \cdot 10^{-3}$
OT3	390.165	$2.5911 \cdot 10^{-3}$

Tabella 3.2.1 Optrodes' temperature sensor coefficients.

How then is the resistance value of the Pt filament measured? A 4-wire measurement is performed using a Keithley 2100MM multimeter (Keithley Instruments Inc., OH, USA). In the following figure 3.2.4, it can be noticed how this sort of resistance measurement is carried out.

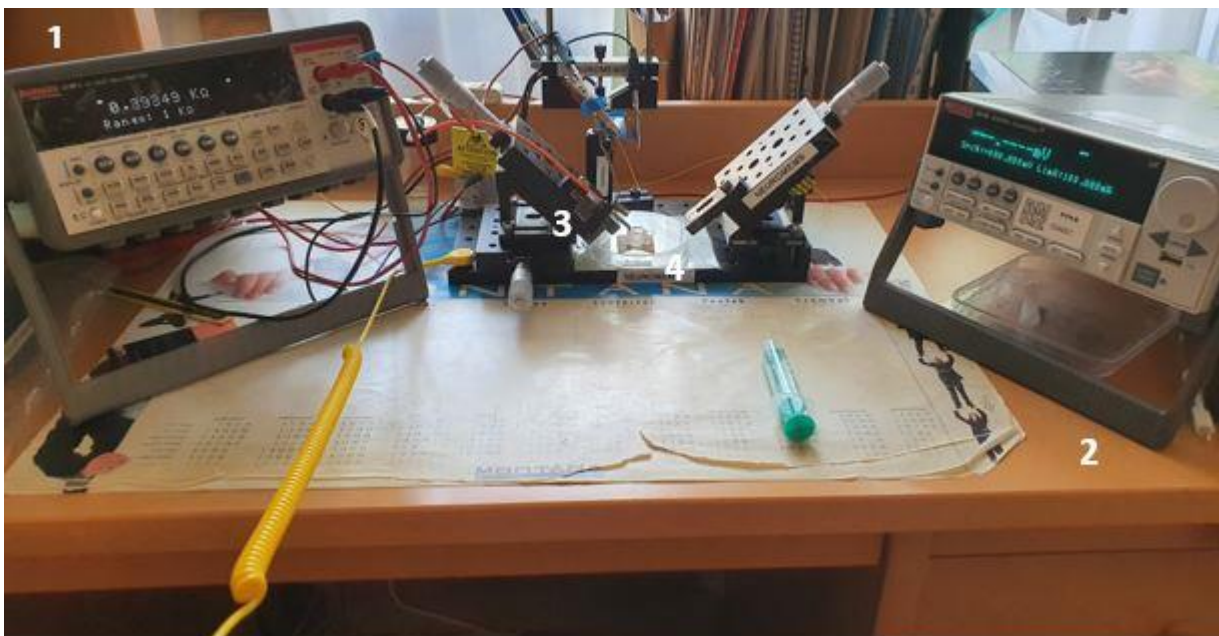


Figure 3.2.4 The 4-wire resistance measurement setup and the whole arrangement. (1) Keithley 2100MM Multimeter in 4-wire resistance measurement configuration. (2) Keithley 2635A Source-measure Unit. (3) The optrode microdevice. (4) 2 ml of tap water.

The measurement range is set to 1 k Ω , and the integration time of the multimeter's A/D converter is set to 0.4 ms (measurement rate set to 0.02 Power Line Cycle PLC).

As with any measuring instrument, the value measured by the multimeter will be affected by uncertainty. The absolute accuracy δR_x of the measured value (R_x) will be, as described in the multimeter datasheet, expressed as follows:

$$R_x \pm \delta R_x = R_x \pm (\% \text{ of reading} + \% \text{ of range}) = R_x \pm (0,015\% R_x + 0,002\% 1 \text{ k}\Omega)$$

with:

- δR_x = absolute accuracy of the measured value;
- R_x = resistance value measured by the multimeter;
- 1 k Ω = the measurement range.

The accuracies of R_0 , α and those related to the leads used to carry out the measurements were considered negligible.

The measurement accuracy's role will prove to be a crucial part of software development, particularly in the temperature measurement part, during each closed-loop iteration. However, this will be an in-depth issue later, during the detailed description of the software.

3.3 The chosen control system

Now a broad vision of the proposed system is presented.

The control system provides for the sharing of some elements, supervised by software implemented in Matlab. This software has the task of making available the supply current necessary for the IR laser diode to work (the external source of the system), correctly driving the Source-measure Unit (SMU) of Keithley 2635A (Keithley Instruments Inc., OH, USA). The value of this DC current supplied by the SMU determines the optical output power of the light emitted by the IR laser (in turn, as already explained, coupled to the multimode fibre-optrode system) and, consequently, of that emitted by the optrode's tip (more details about what optrode interacts with are observable in figure 3.3.1).

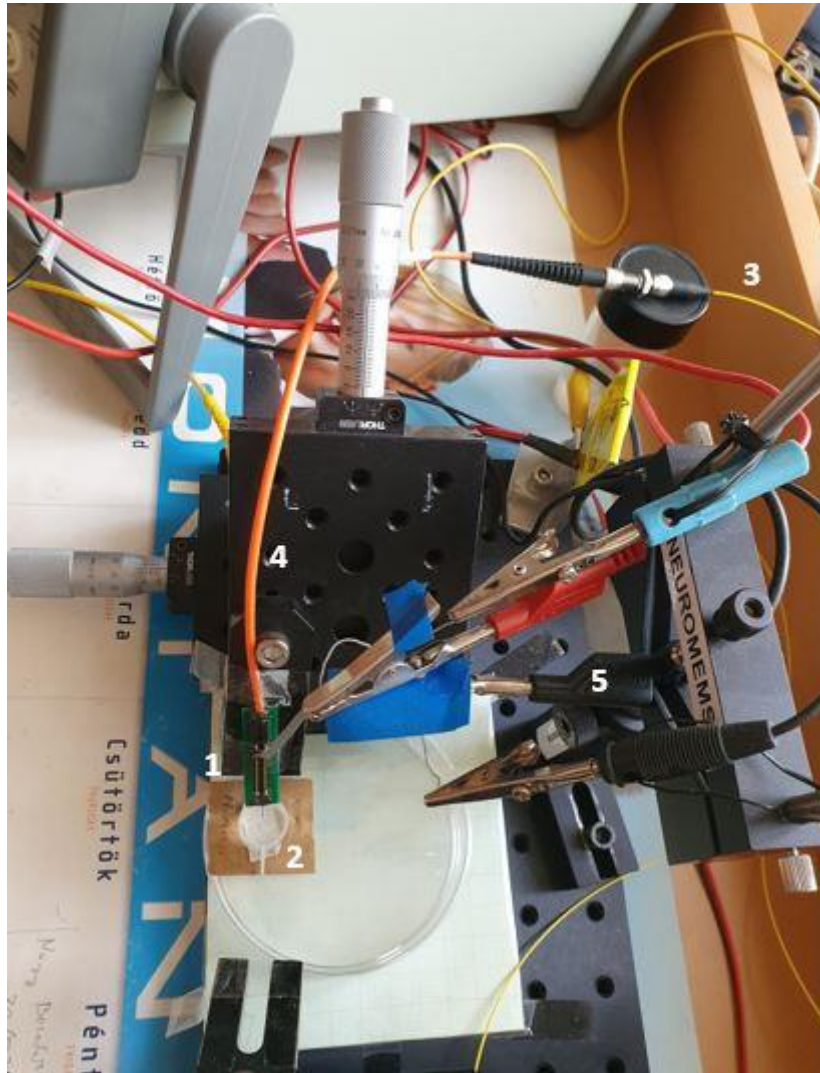


Figure 3.3.1 Experimental closeup that pictures the main elements interacting with the optrode. (1) The packaged optrode device. (2) 2 ml of tap water. (3) The Thorlabs IR laser diode. (4) The multimode optical fibre. (5) All the leads exploited for the Pt filament's resistance measurement.

The value of the current will mainly depend on what is measured by the 2100MM multimeter (supervised by the Matlab software as well) according to the 4-wire measurement method of the integrated Pt filament's resistance. All the acquired resistance values will be saved in a directory chosen by the user, when the control system is switched on, in ".csv" format.

The proposed "closed chain" is the following: the operation control of the Keithley 2635A based on the feedback of Keithley 2100MM, all implemented in Matlab.

The diode's supply DC is, therefore, the system's "output controller" to be iteratively modified based on feedback, which will be the local temperature value of the brain tissue cyclically measured and monitored for the entire life of the closed-loop. This way of working is used to be the same in any kind of continuous process until the set goal is achieved. Nevertheless, what, in this case, would be

the "objective" to be achieved? According to the made choices, it coincides with the input itself which, through the user, "sets in motion" the entire loop. Through a Graphical User Interface (GUI) suitably implemented with the software, the user can set the local temperature (expressed in °C) that the area radiated by the optrode will have to assume at the end of supply current increase process and the maximum time (expressed in s) for which that same area can remain, continuously, exposed to that temperature: reaching (or exceeding) this maximum time (which in other words, will correspond to a certain number of consecutive cycles during which the tissue is kept at the so-called "target temperature") will be the sufficient and necessary condition, if the target temperature is above a threshold value of 40 °C[7], to deactivate the communication with the instrumentation driven by the software and terminate a loop which, otherwise, would risk causing thermal damages to the irradiated tissues. If such input parameters are correctly fulfilled, but the edited target temperature is below the 40 °C threshold, the IR illumination will be temporarily disabled (laser diode supply current equal to 0 mA) without exiting from the system, as long as the measured temperature will not be lower than the target one again. During this sort of transitional pause period, system will perform local temperature measurements anyway.

The target temperature value, set by the user, it will therefore be used by comparing it cyclically to the temperature value indirectly measured by the Pt filament through an error calculation ΔT which should ideally assume, after a certain number of cycles, a null value. The ΔT error, simply given by the difference between the target temperature value and the one measured by the microdevice, if zero will undoubtedly mean that the irradiated tissue area reaches the desired local temperature when the system is switched on control.

The higher the supply DC, the greater the optical output power of the optrode and the more significant the temperature difference made to the area irradiated by the microdevice with respect to its starting temperature at the time of system activation. For these reasons, in order to achieve in a targeted and safe manner the temperature desired by the user, design choices have been made for which the increase in the current that supplies the diode is gradual, cycle after cycle. Doing so, both the optical output power and the temperature increase are gradual as well: this will guarantee the controlled achievement of the "target temperature".

As a closed-loop system, once the control system begins a new cycle, the controller output will depend on the error related to the current iteration as well as the error referred to the previous cycles.

In fact, since the IR illumination starts until a stop or pause condition, the value of the current delivered by the SMU during the succession of cycles can only increase, compared to its starting

value, never decrease. Then, this value will also depend on the previous history of the irradiated area, in terms of perceived temperature. This is an example of how a proportional but also integral action is implemented on the control process.

Figure 3.3.2 schematically sums up all the communication steps that elapse between the various participants of the proposed closed-loop control.

Now a more detailed description of the software structure and the related project choices is presented in the following chapter.



Figure 3.3.2 The operational flow of the proposed closed-loop control in full operation.

4 Detailed introduction of the control system

4.1 The Graphical User Interface (GUI)

The GUI is the primary tool that allows the user (who can be, for example, a brain researcher) to interact with the control software developed in this thesis.

The correct use of this interface (figure 4.1.1 shows what user can see when the GUI has just been opened) and therefore, correct management of the control system is guaranteed by respecting the order in which the steps below are listed.

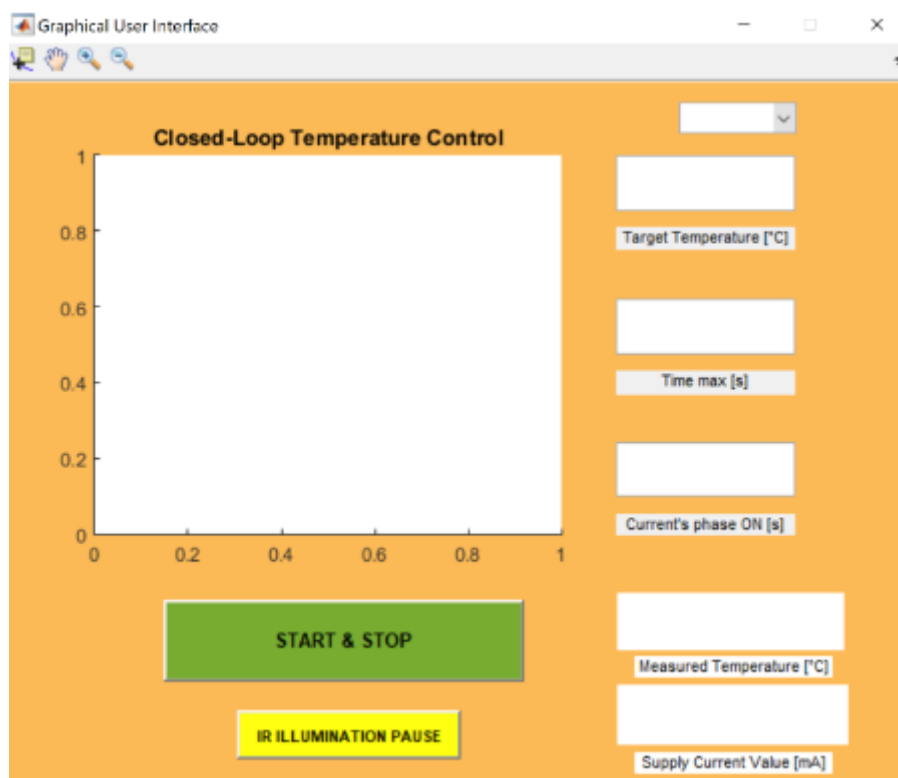


Figure 4.1.1 The GUI before setting all input parameters.

1. Use the popup menu at the top right, as shown in figure 4.1.2, in order to choose the correct optrode temperature sensor parameters (OT1, OT2 or OT3).

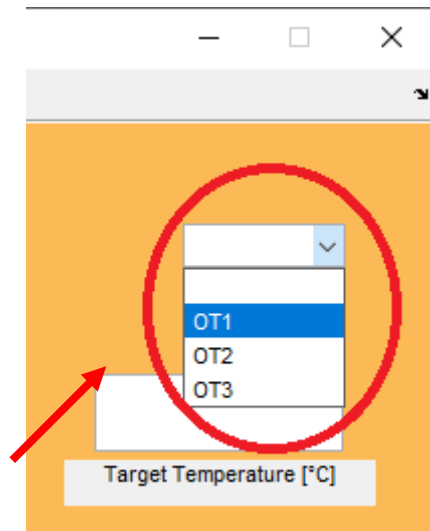


Figure 4.1.2 The optrodes' popup menu.

2. First edit the "Target Temperature" at which the irradiated tissue must arrive (in ° C), as shown in figure 4.1.3.

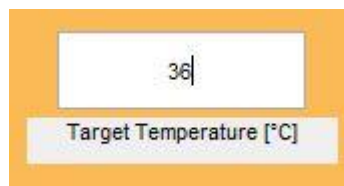


Figure 4.1.3 The user-editable Target Temperature box.

3. As indicated in figure 4.1.4, edit the maximum time for which the tissue must be continuously kept at the target temperature (in s).

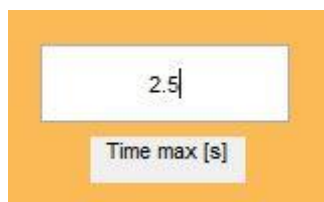


Figure 4.1.4 The user-editable maximum exposure time box.

4. Edit the phase "ON" of the diode's supply current waveform (in s) which will correspond to the duration of continuous irradiation by the optrode at a specific optical power, during each loop cycle (editing example in figure 4.1.5).

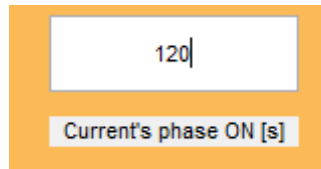


Figure 4.1.5 The user-editable phase "ON" of the diode's supply current box.

5. Once these few parameters have been set, press "START & STOP" toggle button to activate the closed-loop control. During each cycle, the local temperature value will be measured, which will appear both numerically (expressed in °C) in the "Measured Temperature" box at the bottom right, and graphically in the Time vs Temperature plot, placed in the centre of the GUI. There are also available tools in order to manage the pictured live plot: data tips, pan, zoom in and zoom out. During the loop's operation, it is also possible to appreciate, in real-time, in the box at the bottom right "Supply Current Value", the value of the current (expressed in mA) that is supplying the IR diode. Figure 4.1.6 shows an example of the boxes' real-time updating during the control system's operation.

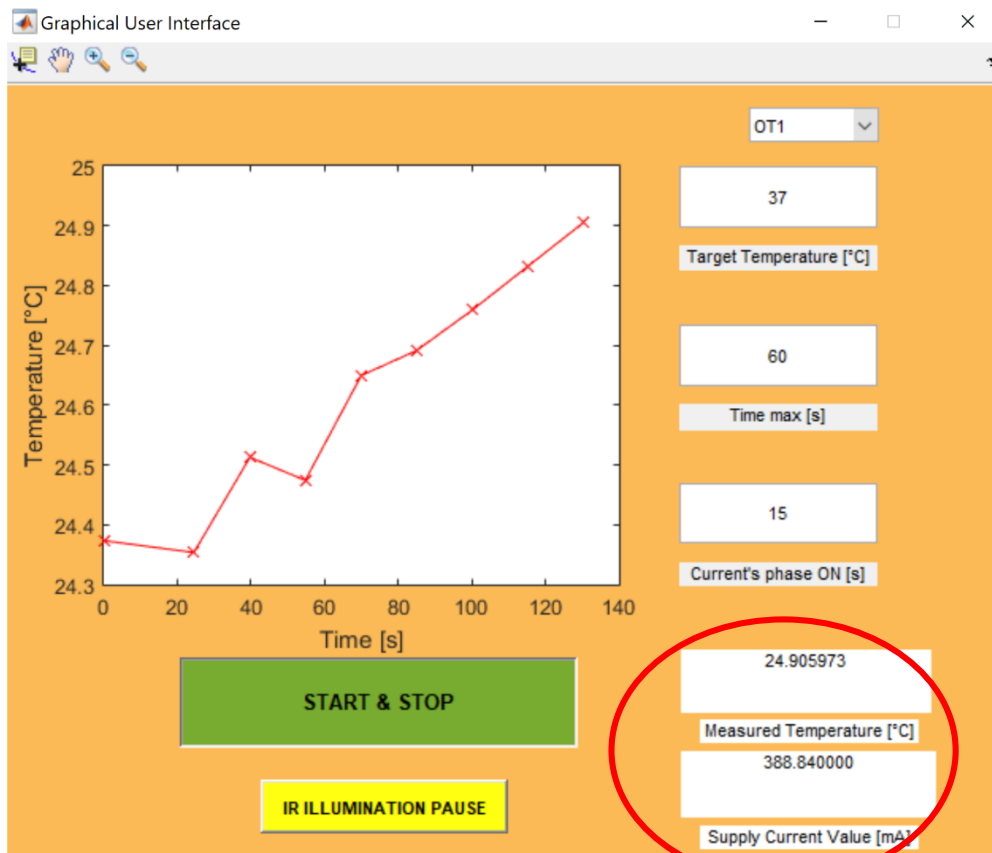


Figure 4.1.6 Updated boxes of measured temperature and supply current value during the system operation.

6. Press the “IR ILLUMINATION PAUSE” toggle button to suspend the optrode’s IR illumination temporarily at any time during the control system operation, without closing the instrumentation communication. In fact, if this function is enabled, the system will continue to perform temperature measurements delivering a supply current of 0 mA to the SMU, during every loop cycle.

7. Press the "START & STOP" toggle button again to switch off the system at any time at the end of the current loop cycle, thus interrupting the communication with the instrumentation piloted by the software.

4.2 The start of the closed-loop control and the overall program

Once the "START & STOP" button is pressed, the developed control system is then started.

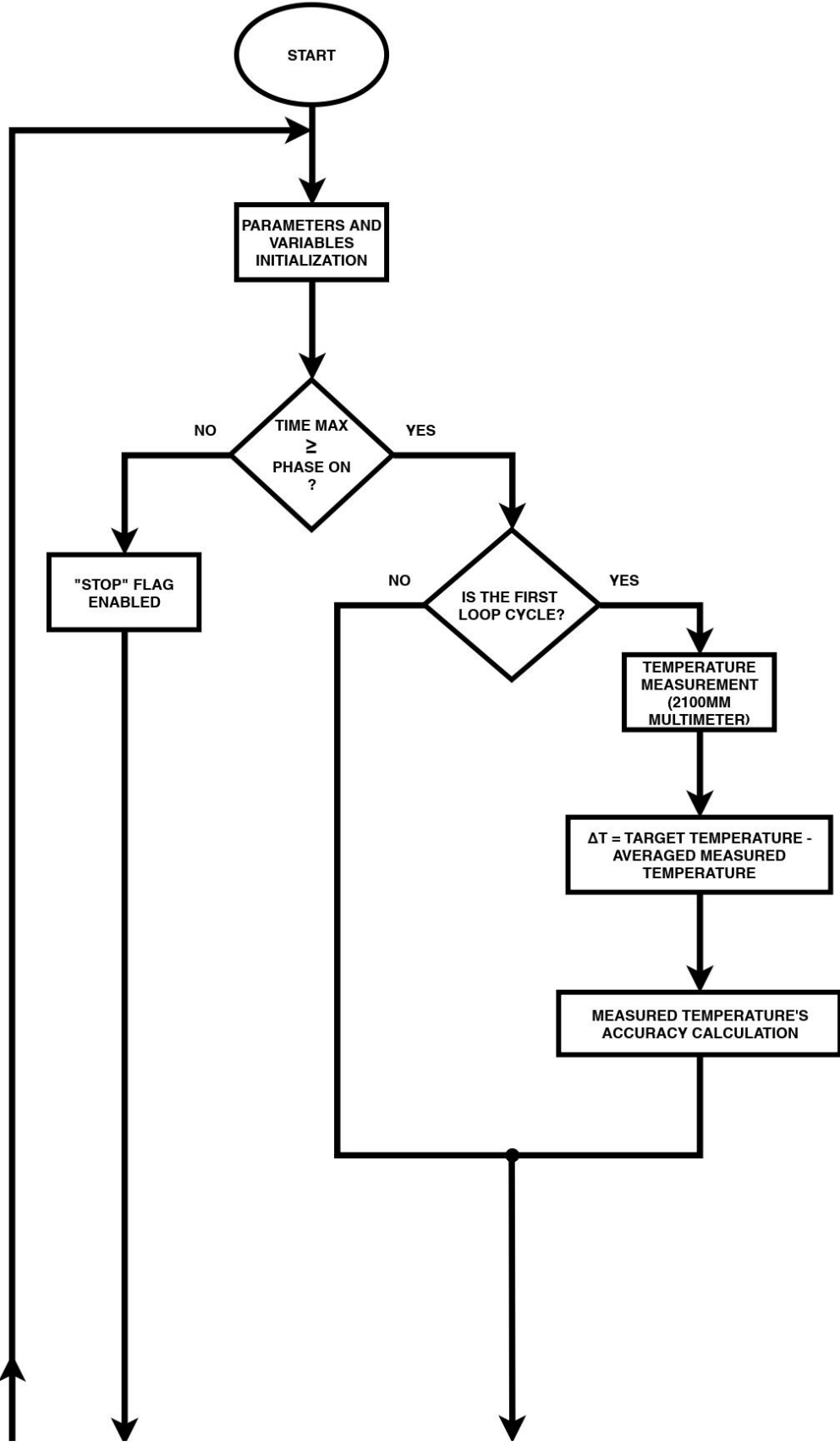
First of all, all the variables, counters, flags useful for the correct functioning of the software are initialized, including the buffers useful for storing the resistance measurements made with the Keithley 2100MM and for representing the "Time vs Temperature" plot. In the same way, the Keithley 2635A work parameters are suitably initialized before the actual software loop begins.

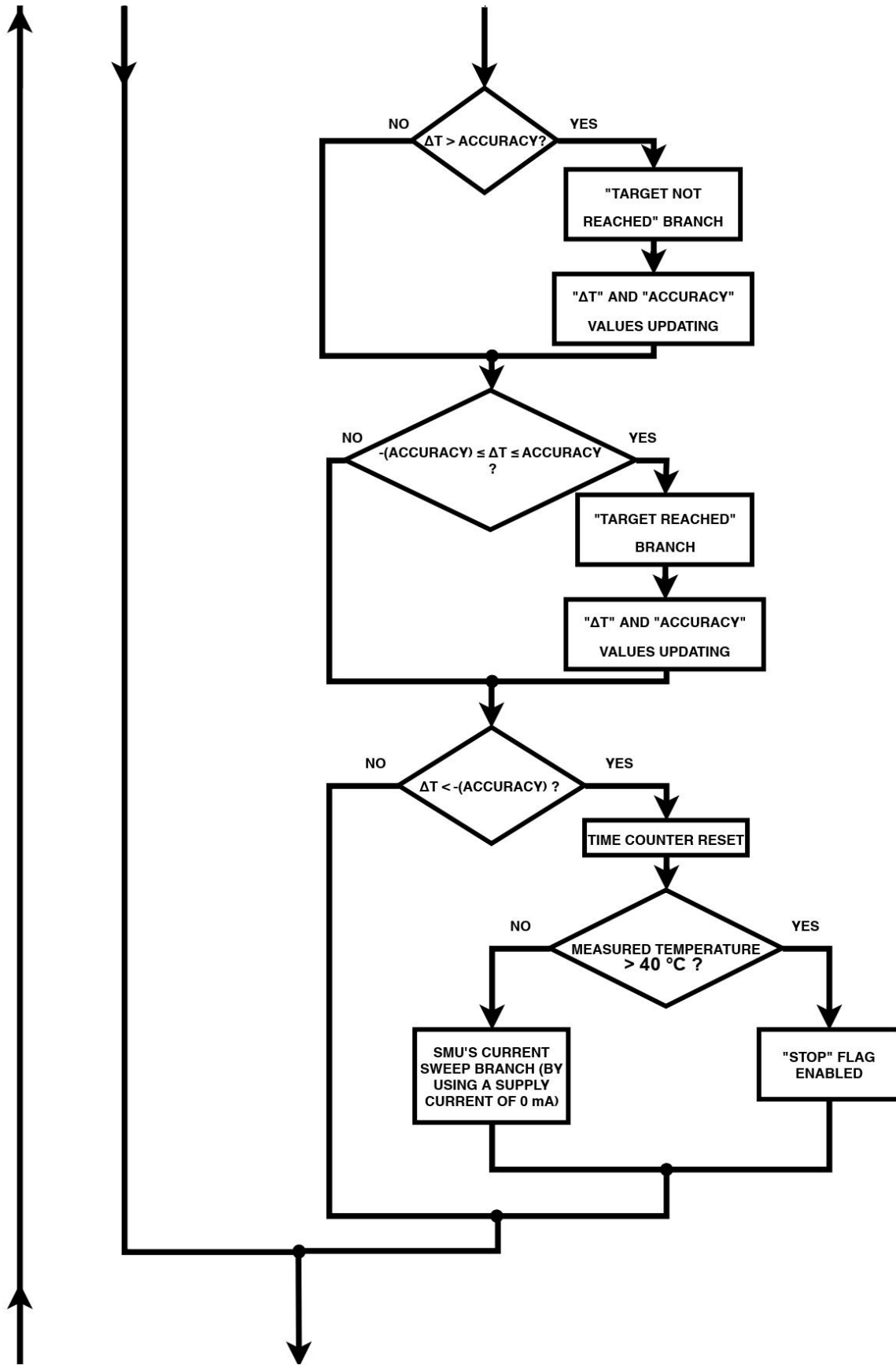
When the main loop is activated, the software must first carry out communication with the multimeter alone, therefore not in conjunction with the irradiation phase performed by the optrode. As soon as while loop start conditions have been met, the software starts taking resistance measurements which will be saved on Keithley 2100MM internal memory. After that, it reads these values via USB and stores them to a vector buffer. The average time that elapses between one acquisition and another one is approximately 40.725 ms. During each step of measuring and acquiring the resistance values of the integrated sensor, a batch of five measurements is obtained, which is why the overall average time used for resistances measurements and acquisitions is about 204 ms. When a 5-measurements batch is finally obtained, the measured results are moved from the vector buffer to a ".csv" file (once initially the user activates the GUI, a dialogue box is automatically opened for deciding the “.csv” file’s name and destination directory).

All the measurement batches acquired after the first one will be obtained during the last part of the tissue irradiation phase so that all the loop cycles following the first will have a duration equal to the period of the waveform of the supply current used for the IR diode (“Current’s phase ON” [s]). The first absolute cycle will therefore last approximately 204 ms and so shorter than the subsequent ones due to the acquisition of the first batch outside the irradiation phase. Since, as will be explained later,

the waveform used will be characterized by a duty cycle of 100%, each loop cycle following the first one will have a duration precisely equal to the “ON” phase of the supply current. For these reasons, the software performs a preliminary check which, in the event of a negative result, would cause the control system to terminate its operations prematurely. Indeed, if the maximum time of exposure to the “Target Temperature” is less than the phase "ON" value, this would lead to a case that is not admissible by the software as the minimum time at which the tissue can be exposed to the target temperature is one loop cycle’s duration. The minimum duration of exposure to the target temperature coincides, for the design choices made, with the duration of a single irradiation cycle (which correspond, as already said, to the “ON” phase of the supply current).

Figure 4.2.1 represented in the next three pages pictures the flowchart that allows a general view of what the software can do, from the moment the "START & STOP" button is pressed until one of the "stop" conditions are met.





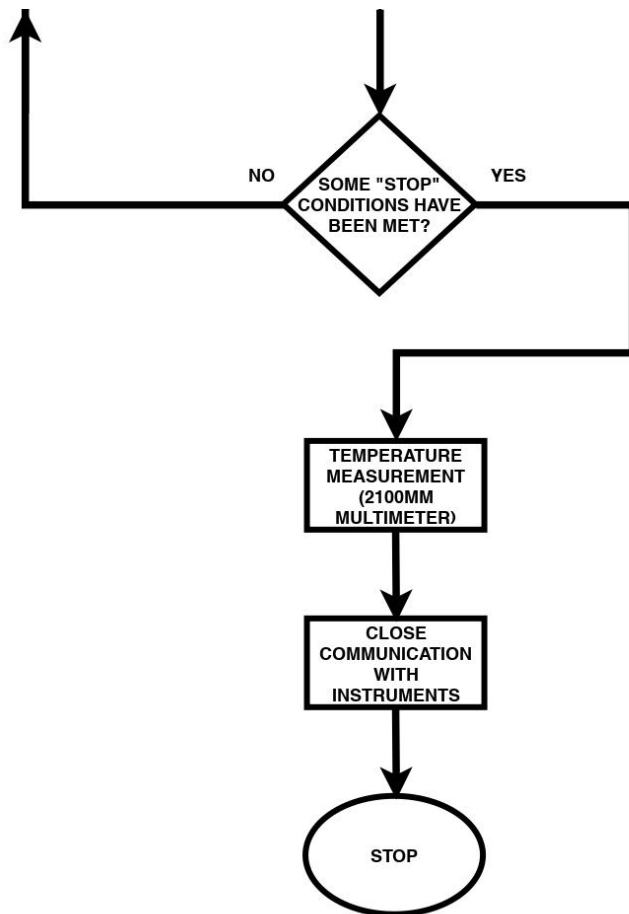


Figure 4.2.1 The overall software flowchart.

As it is possible to appreciate by observing the flowchart, the values measured by the multimeter are used in such a way as to obtain, as a final result, an averaged value of the local temperature. The software, starting from this latter value, will be able to obtain the error ΔT concerning the target temperature value chosen by the user, together with the respective accuracy linked to the measurement action of the multimeter.

The value of the error ΔT establishes the possible beginning and the modalities of the communication with the Keithley 2635A SMU to deliver the IR diode supply current or the "forced" exit from the control system, finding the "stop" condition.

All buffers and useful variables are cleaned every time a temperature measurement operation is performed.

4.3 Source-measure Unit's parameters settings

The SMU (Source-measure Unit) is an instrument that combines source and measurement capabilities in a single instrument. Its source features are used to supply the IR diode by providing a DC driving current.

Here described all the choices made for what concerns the communication with Keithley 2635A SMU, in order to obtain as a final goal a correct IR irradiation by the optrode.

As regards the supply current's waveform, this is theoretically characterized by an "ON" and an "OFF" phase (so we can speak of a pulsed current). In this case, however, we have chosen to opt for a D.C. duty cycle of 100% (this means with no "OFF" phase) whose "ON" phase is set directly by the user through the GUI, during the control system initialization phase. By doing so, it is ensured that continuous irradiation with a duration precisely equal to the "ON" phase can undoubtedly allow us to appreciate, during an individual loop cycle, the thermal transient obtainable with that specific power, until reaching stationarity[6].

For example, a continuous power supply of the diode for 2 minutes ("ON" phase = 120 s) and, namely, continuous irradiation of 2 minutes by the optrode, at a specific optical power, allows the achievement of an almost stable and stationary local temperature by the tissue. Furthermore, this does not lead to responses that can be linked to excessive thermal stress of the irradiated tissue, such as astrocytic responses. Besides, it has been shown that continuous irradiation of this type (i.e. lasting from seconds to minutes) has excellent potential in the analysis of neural networks[7]. The proposed waveform of the current therefore suggests, with this duty cycle D.C., how to avoid that the irradiated tissue returns to its baseline temperature, during the various irradiation loop cycles of the control system.

As the graph pictured in figure 4.3.1 suggests, the temperature variation induced by IR illumination, once irradiation is stopped, generally tends to cancel out very quickly.

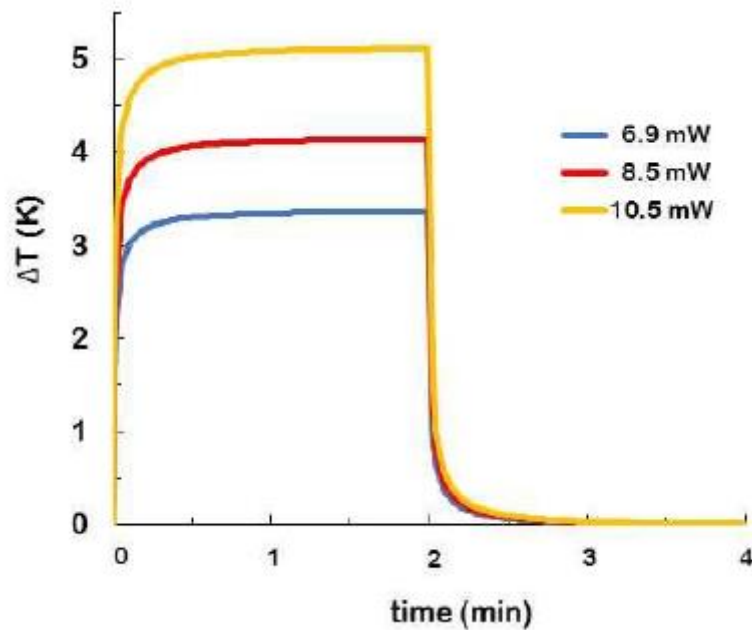


Figure 4.3.1 Horváth et al.[6] Infrared irradiation of rat's cortical neurons at 1600 μm of depth: simulated temporal change of temperature in the vicinity of the integrated temperature sensor of the optrode in the case of different applied optical powers. Duration of the IR irradiation: 2 minutes.

Hence, by choosing a D.C. of 100%, it is guaranteed that the duration of each loop cycle, from the moment in which the first irradiation phenomenon occurs by the microdevice, coincides precisely with the "ON" phase of the IR diode supply current's waveform. This loop cycle's lifetime is because, as already mentioned, the measurements made by the multimeter after the first absolute measurements (those that are made as soon as the system is switched on) are performed while irradiation is in progress.

At the first useful loop cycle, during which it will be necessary to power the diode, a starting current will be supplied which, in turn, will be responsible for the first "thermal jump" of the irradiated tissue. If the thermal jump caused by the delivery of this starting driving current will not be sufficient to reach the "Target Temperature" set by the user (and so the optical output power related to will turn out to be insufficient), during each cycle following the first one, an extra ΔI will be added to the previously "I" supplied current value (the idea is summed up by figure 4.3.3). This addition will result in higher driving current, in order to guarantee an optical power increase and thus a further thermal jump, reaching cycle by cycle at the desired temperature and object of study by the user.

Critical data from Thorlabs IR diode's datasheet have been partially used to be lead with a careful eye towards correct choices concerning the starting current I_{start} and the extra value ΔI which SMU must deliver during every irradiation cycle after the first one.

Parameter	Symbol	Value	Unit
Fibre output power	P_{op}	80.0	mW
Operating current	I_{op}	359.6	mA
Operating voltage	V_{op}	1.44	V
Threshold current	$I_{threshold}$	41.8	mA
Slope efficiency	$\Delta P/\Delta I$	0.23	mW/mA
Center wavelength	λ	1555.0	nm

Table 4.3.1 Most relevant parameters of the Thorlabs LPSC-1550-FG105LCA-SMA laser diode's datasheet. Data obtained during a CW (Continuous Wave) test ($T_{CASE} = 25\text{ }^{\circ}\text{C}$)[24].

Parameter	Ratings	Unit
Laser diode current*	500	mA
Optical output power*	60	mW
Laser diode reverse voltage*	2	V
Storage temperature	-10 to +65	$^{\circ}\text{C}$
Case temperature	0 to +50	$^{\circ}\text{C}$

Table 4.3.2 Thorlabs LPSC-1550-FG105LCA-SMA laser diode's absolute maximum ratings. *Data obtained under CW test, $T_{CASE} = 25\text{ }^{\circ}\text{C}$ [24].

Another essential support was provided by the experimental data of Horváth et al.[6] regarding the irradiation, via optrode, at the level of the rats' neocortex. The main reason that made it possible to exploit this type of data lies in having noticed that there is an approximately linear relationship between the optical output power of the emitted light and the thermal difference that this irradiation induces on the tissue.

First, it was tried to find for the starting current I_{start} , a value through which the optical output power could induce a thermal jump ΔT of $1\text{ }^{\circ}\text{C}$. Thermal variations of this magnitude result in significant functional alterations in various areas of the nervous system[23], indicating the high sensitivity of the brain[7].

As indicated in the diode's datasheet, the slope efficiency is equal to:

$$\frac{\Delta P}{\Delta I} = \frac{P_2 - P_1}{I_2 - I_1} = 0.23$$

with:

- ΔP = optical output power variation;
- ΔI = driving current variation.

$P_1 = 0$ mW and $I_1 = 0$ mA because the diode's starting status is "off". The mean P_2 value is obtained by averaging the optical power values useful to obtain a $\Delta T = 1$ °C in the rat's cortical area at 1300 μ m and 1600 μ m of depth, respectively:

$$\overline{P_2} = \frac{6.9 + 2.125}{2} = 4.5125 \text{ mW}$$

Then:

$$\frac{\Delta P}{\Delta I} = \frac{\overline{P_2} - P_1}{I_2 - I_1} = \frac{P_{start} - 0}{I_{start} - 0} = \frac{4.5125 - 0}{I_{start} - 0} = 0.23$$

$$I_{start} = \frac{4.5125}{0.23} = 19.619 \text{ mA}$$

I_2 is the theoretical starting current useful to increase of 1 °C the irradiated tissue temperature.

However, observing table 4.3.1, this current value just obtained turns out to be too low, as the minimum operating current (the so-called "threshold current" $I_{threshold}$) is equal to 41.8 mA. The optical power obtainable is then achieved using $I_{threshold}$:

$$\frac{\Delta P}{\Delta I} = \frac{P_2 - 0}{41.8 - 0} = 0.23$$

$$P_2 = 9.614 \text{ mW}$$

By using the experimental data which belong to the rat's neocortex areas again, the averaged ΔT value obtainable with this optical power is achieved as follows:

$$\overline{\Delta T_{MEAN}} = \frac{1.3 + 3.5}{2} = 2.4 \text{ °C}$$

This last value is the average temperature difference obtainable by delivering an I_{start} starting current equal to $I_{threshold}$.

However, it should be emphasized that the choice of $I_{threshold}$ as starting current cancels the margin of error to a correct diode power supply: in fact, the $I_{threshold}$ plaque's value may, over time, change due to the ageing of the diode material.

Besides, using the slope efficiency of the datasheet in the design calculations as just described, was not an optimal choice since this ratio does not take into account the power losses that occur during the propagation of light due to the effects of optical fibre and the Si waveguide. It is therefore shown that by obtaining a new ratio experimentally, it is possible to obtain calculations with more robust results concerning these "collateral" phenomena. This robustness consists of especially obtaining an I_{start} value much higher than the datasheet's value of $I_{\text{threshold}}$ and so a more effective current value against the ageing phenomena of the diode.

The $\frac{\Delta P}{\Delta I}$ mean values were first obtained for each of these curves represented in figure 4.3.2 (and therefore for each of the three inspected optrodes), considering only reliable data relating to optical powers up to 10 mW, as above this value the data cannot be more considered consistent due to saturation phenomena of the optical power meter's sensor.

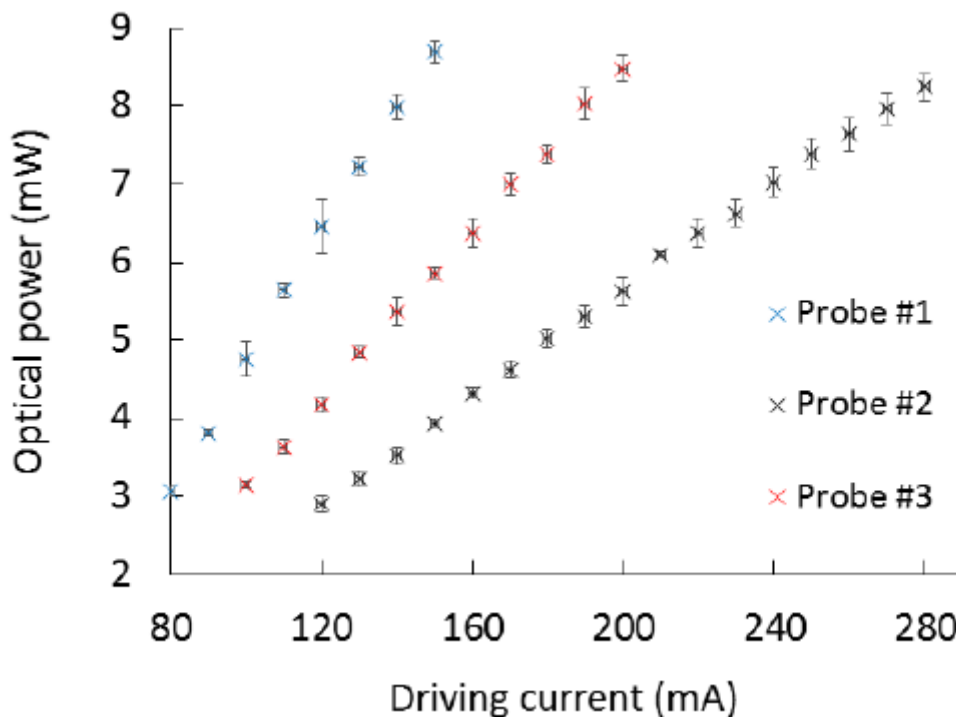


Figure 4.3.2 Horváth et al.[6] A characteristic change in optical power vs driving current of laser diodes, for three different probes' features. Measurements were performed at the probe tip using an absolute power meter.

The $\frac{\Delta P}{\Delta I}$ mean ratios for each of the three optrodes are so as follows:

Probe #1 [mW/mA]	Probe #2 [mW/mA]	Probe #3 [mW/mA]
0.082431818	0.0534	0.037277778

Table 4.3.3 Slope efficiency's mean values of the three inspected optrodes.

The approximate and unique value for all three optrodes, given by the average of the values represented in Table 4.3.3 and which will be used in the next project calculations, is equal to:

$$\frac{\Delta P}{\Delta I} = 0.058$$

Now proceed with repeating the calculations in order to obtain the correct I_{start} value.

$$\overline{P}_2 = \frac{6.9 + 2.125}{2} = 4.5125 \text{ mW}$$

Then:

$$\frac{\Delta P}{\Delta I} = \frac{\overline{P}_2 - P_1}{I_2 - I_1} = \frac{P_{start} - 0}{I_{start} - 0} = \frac{4.5125 - 0}{I_{start} - 0} = 0.058$$

$$I_{start} = \frac{4.5125}{0.058} = 77.8 \text{ mA}$$

Given this, as already mentioned, with these changes, it is noted that:

$$77.8 \text{ mA} > I_{threshold}$$

thus obtaining an increase of the I_{start} of 86% with respect to the $I_{threshold}$.

Regarding the ΔI choice, a value for which the target temperature is reached, cycle by cycle, with a further thermal jump ΔT of 0.5 °C compared to the temperature reached by the tissue during the previous loop cycle, has been chosen. An increase of 0.5 °C is still considered an optimal and compelling value for gradually approaching the target temperature, thus obtaining functional alterations that are however not negligible.

Mediating once again the experimental values available on the irradiation via optrode of the cerebral cortex of rats at 1300 μm and 1600 μm depth, the mean ΔP useful to obtain this ΔT is thus obtained:

$$\overline{\Delta P} = \frac{3.45 + 1.06}{2} = 2.255 \text{ mW}$$

Always by using the new slope efficiency previously obtained:

$$\frac{\overline{\Delta P}}{\Delta I} = 0.058$$

$$\Delta I = 38.88 \text{ mA}$$

So $\Delta I = 38.88 \text{ mA}$ it is the extra-value that the SMU must add to the current delivered during the previous loop cycle, during each cycle following the first one, in order to reach step by step the user-edited target temperature.

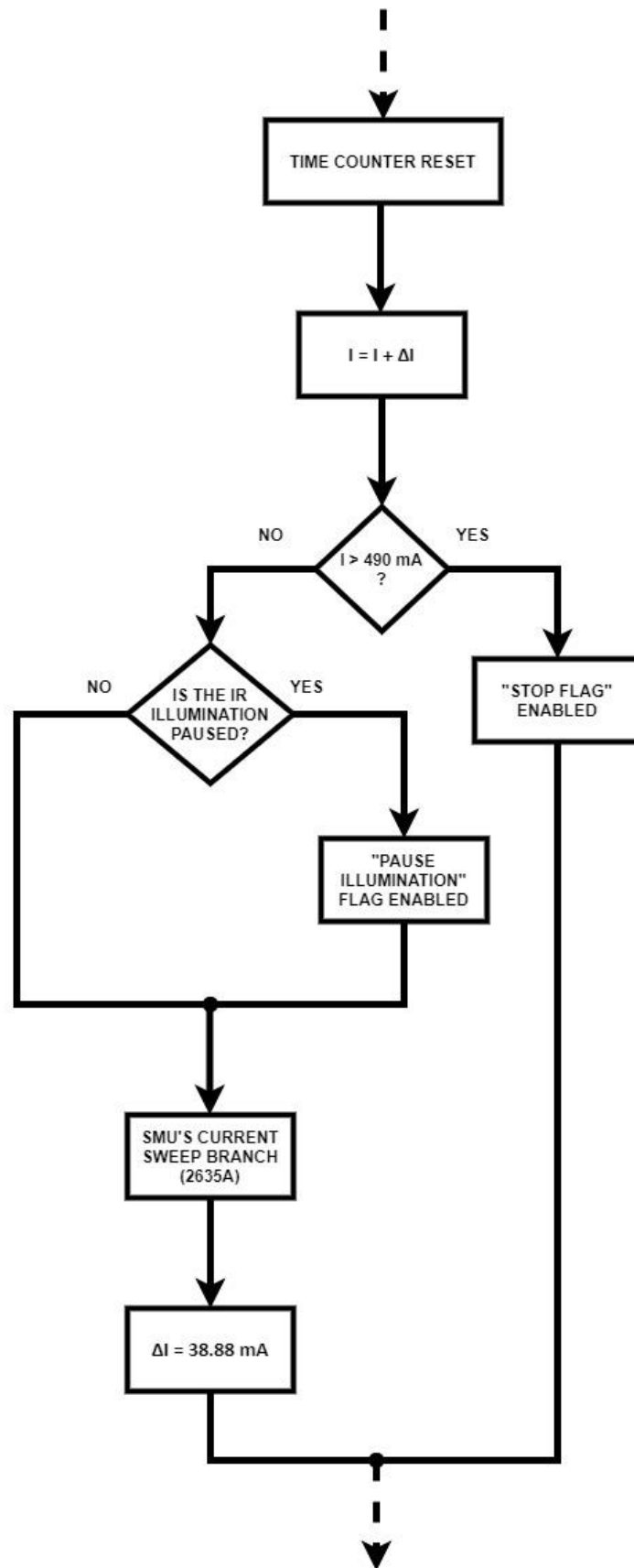


Figure 4.3.3 "Target not reached" branch. Flowchart indicating the program branch in which the target temperature still has not been reached. So if the maximum laser diode current has not been exceeded, SMU communication can be activated.

The actual communication with the instrument is now described. The lines of code, within Matlab space, related to driving the SMU are written using the LUA programming language and define the current sweep setting[24] (all the communication steps are pictured in figure 4.3.6).

The various actions of the SMU are governed and regulated by a synchronized triggering system. Various "event detectors" present in the SMU monitor the triggering events that have been assigned to them and that follow each other during the specific action performances. These triggers are produced by individual "blocks", called trigger objects, following the occurrence of a particular "event" which acts as a "stimulus". It is easy to understand how the various operating blocks of the SMU "dialogue" with each other through the production and reception of trigger pulses, mutually performing their role of trigger objects.

A particular type of trigger object, fundamental for the realization of this software, is the timer. A timer is a trigger object which performs a delay since it receives a trigger event as an external stimulus and, once the delay expires, this timer, in turn, generates a trigger event (which can be exploited as an input event for other objects, look at figure 4.3.4 as an example). In this case, the timers are useful for adjusting the exact duration of the two phases of the driving current waveform delivered by the instrument. In particular, two timers are used in this software: one of them, through a delay performing, guarantees the correct duration of the "ON" phase of the current, that is the pulse width; the other timer is dedicated to the entire period of the current waveform.

The pulse width and period values, expressed in seconds, are chosen and assigned to the two timers.

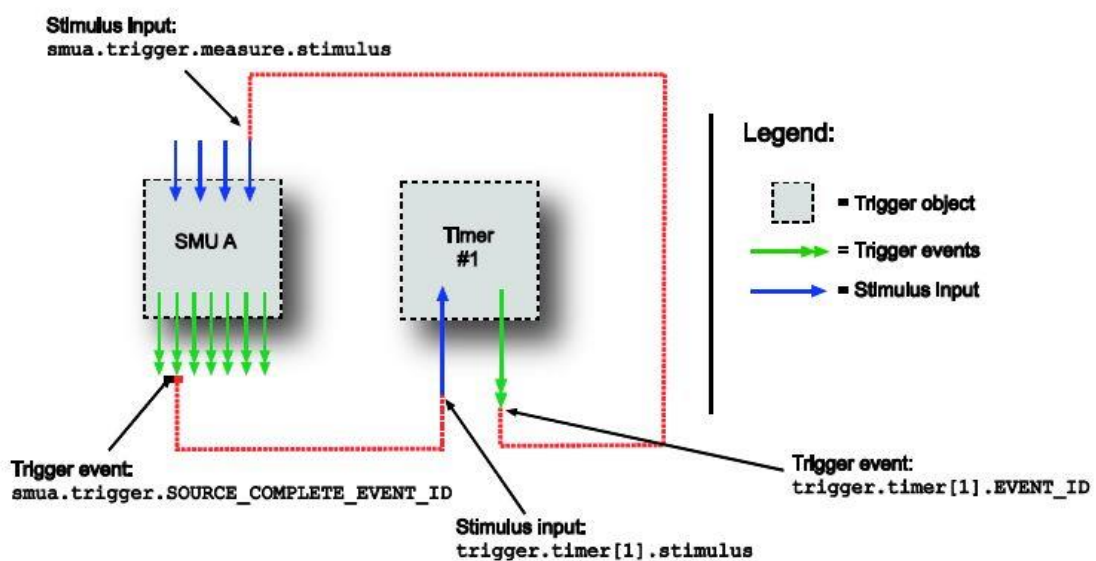


Figure 4.3.4 Example of trigger event useful to let Timer #1 start counting its delay. The external event which activates the timer is, in this example, a trigger that occurred in correspondence of the source action's ending performed by the SMU (as is well known, in this thesis the used source is manifested in the form of current)[24].

For example, the period timer is triggered by an event which, in LUA language, is expressed as "SWEEPING_EVENT_ID". In order to explain what this event corresponds to, it is necessary to introduce what passes under the name of "remote trigger model". The remote trigger model schematically describes the various steps through which the various actions, carried out during the source/measure performances of the SMU, follow each other according to specific timing. In other words, that model dictates the sequence of operation for the SMU when it is configured to perform a sweep[24]. Therefore, in order for each action block of the model to be executed, the corresponding stimulus input captured by the detector assigned to it must occur. If this did not occur, the SMU would ignore that block by continuing its path through the model, towards the next block (and what, in the case of this thesis, happens with the blocks relating to measurement activities, which are therefore not covered).

As it can be seen from figure 4.3.5, during its source/measure performances, the sweep goes through three "levels" that characterize this trigger model:

- idle state: the sweep is not in process;
- arm layer: is the level where a sweep starts but also ends;
- trigger layer: the real source/measure actions occur at this level. In particular, it corresponds to that moment of the current sweep when the actual delivery of the driving current takes place.

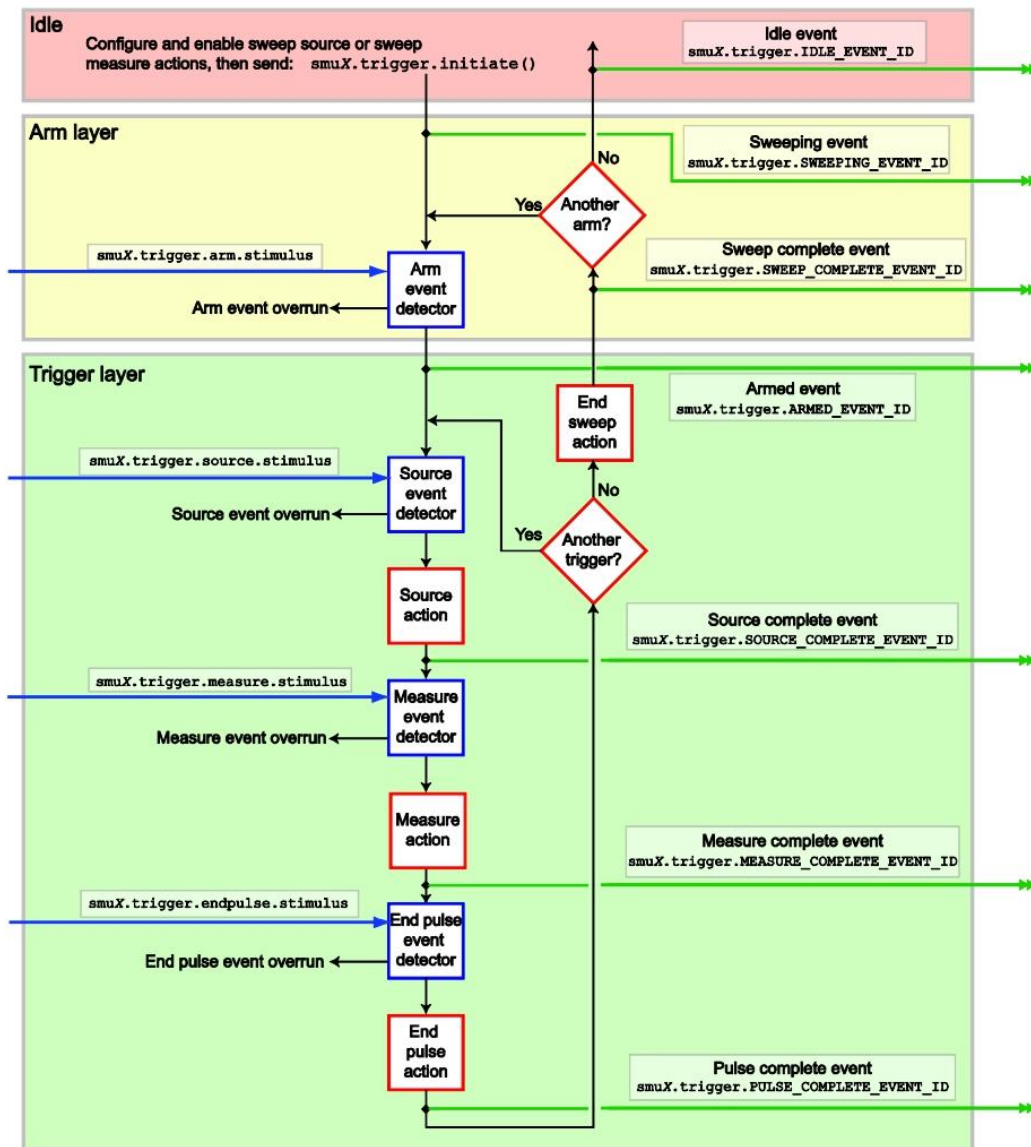


Figure 4.3.5 The remote trigger model.

During the execution of an individual closed-loop control system's cycle, the SMU can, in turn, remain in the arm and trigger layer for more inner-loops, through the use of special counters. For the realization of this software, the SMU will perform only one inner-loop in each of these layers ("arm" and "trigger counts" set to 1).

So returning to figure 4.3.5, the event able to trigger the period timer is a trigger issued in correspondence with the passage of the SMU from the idle state to the arm layer, during the current sweep performing. Other similar settings in the software code are as follows:

- pulse width timer triggered by the period timer;

- synchronization of the end of the current pulse with the pulse width timer trigger (which occurs when the pulse width delay elapses).

In order to guarantee the generation of a trigger by a timer even when it has just been triggered, without waiting for it to be generated only when its delay expires, the so-called "pass-through" mode is enabled in the SMU. This choice ensures that the entire current sweep mechanism is thus perfectly synchronized and effective.

Other important parameters, to be passed to the instrument in LUA language and relating to the current delivered, are the current range and the voltage compliance limit.

For the first, the "auto range" mode which allows the Keithley 2635A to automatically go to the most appropriate range for the current value supplied, has been disabled. Indeed, the current range has been manually set to 490 mA in order to make the software faster while driving the SMU (and so decreasing possible sources of error). This choice does not affect the control system work, because it is sure that values assumed by the supply current certainly range from few tens of mA (typically the diode threshold current) to almost the maximum operational diode current.

As for the output voltage limit of the current source (compliance), the value is set to 2 V.

As previously mentioned in paragraph 4.1, the user can enable and disable the "IR ILLUMINATION PAUSE" toggle button at any time while the CLC system is working. Once enabled, the software will activate an appropriate flag indicating that this alternative modality is running. In order to let the CLC system adapt to this situation, a flag's value check will always be performed before the "SMU's current sweep branch" starts. The successful flag check as activated will force the SMU communication code-block to work by using a supply current of 0 mA, actually letting the system to do only temperature measurements, until the illumination pause is disabled again.

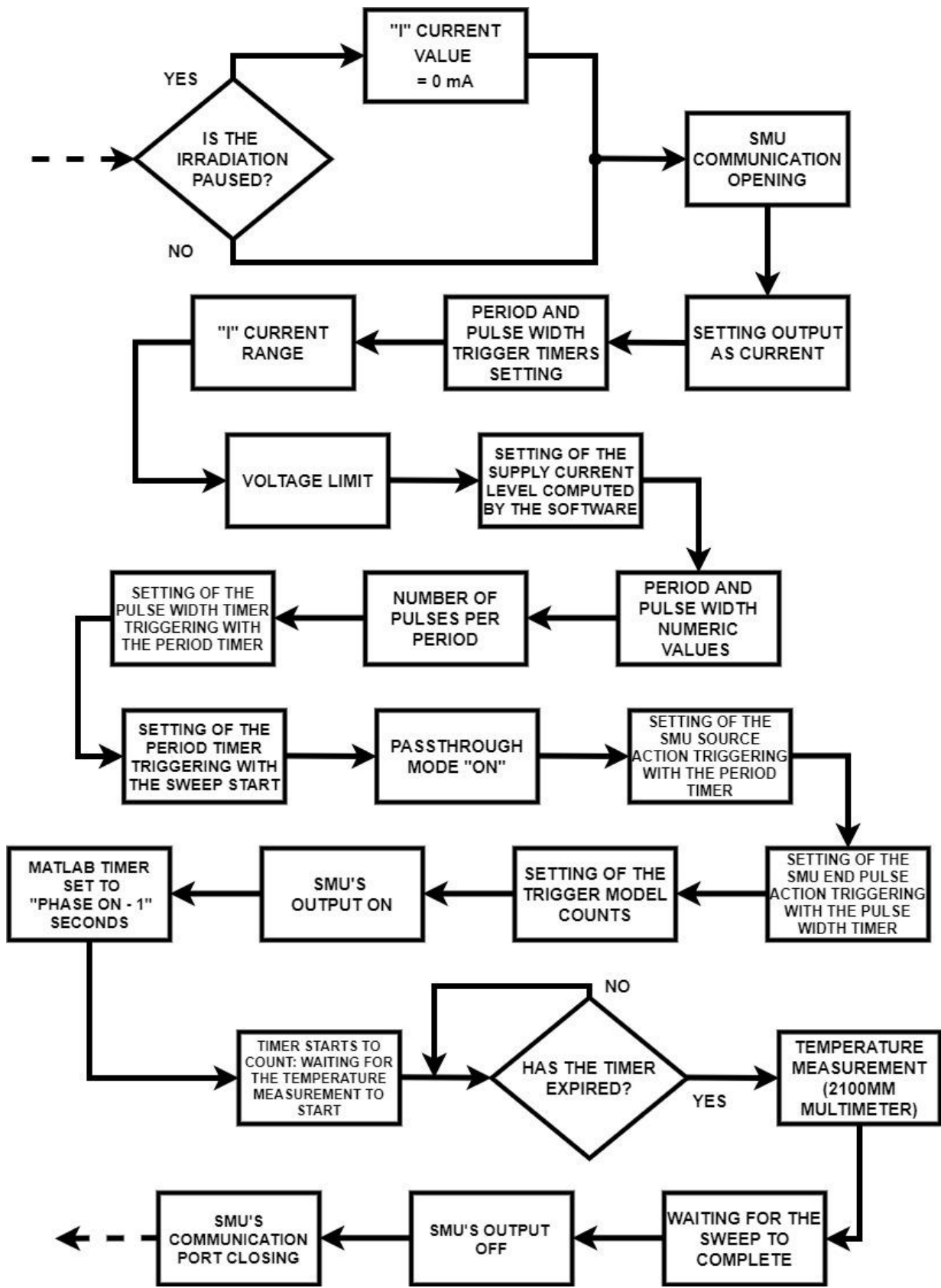


Figure 4.3.6 Flowchart of the SMU's current sweep branch programming.

4.4 The temperature measurement's approach

The temperature measurement is carried out locally to the optrode's tip by using an appropriate conversion of the resistance value of the Pt sensor. The latter one is given by the average of five samples measured and acquired by the Keithley 2100MM multimeter on its internal memory. Each of these five samples is acquired by the multimeter every approximately 40.725 ms, with an overall time useful for obtaining the relative measured temperature value of about 204 ms. It has been demonstrated that a smoothed average of five measured samples can give reasonably good precision results with a quite fast digits refresh[6].

Buffers, variables and flags used for the entire measurement phase performed by the software are cleaned and reset, once the following conditions have been met:

- the five measurements, the values of which are appropriately saved in a “.csv” file located in a directory chosen by the user, have been carried out;
- the five measurements have been mediated between them;
- the aforementioned Callendar-Van Dusen relationship has been used in order to achieve the final value temperature expressed in °C.

Figure 4.4.1 summarizes the whole procedure:

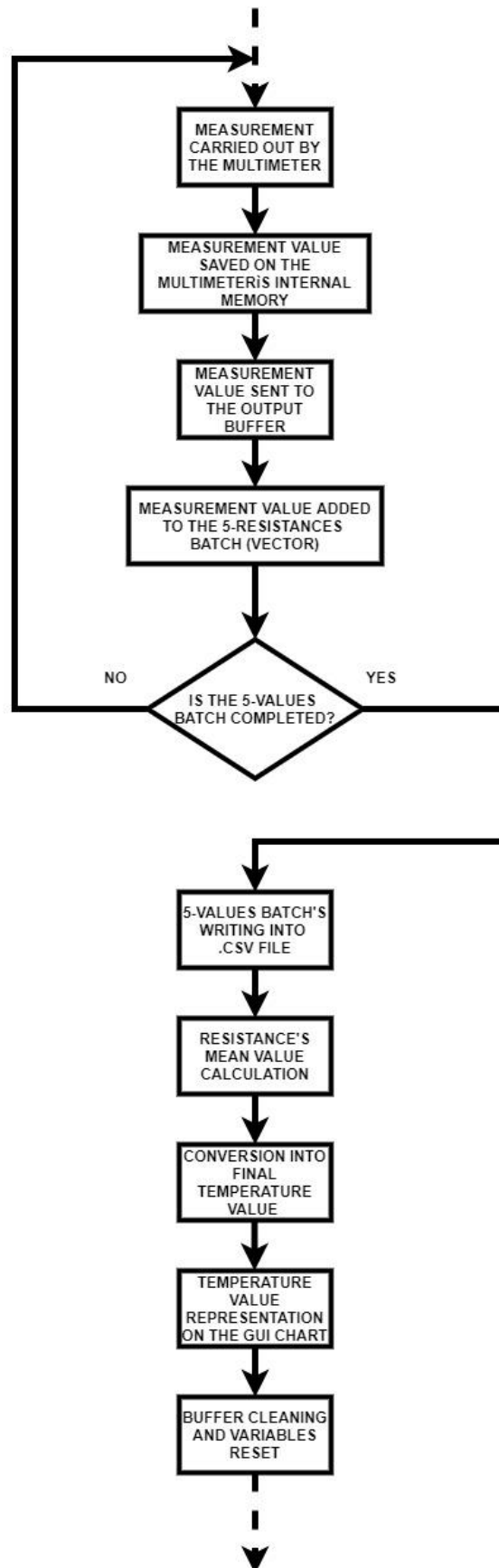


Figure 4.4.1 Flowchart of the temperature measurement phase, performed by using the Keithley 2100MM multimeter.

This operation, cyclically performed by the control system designed in this thesis project, first of all, will take place once the system is switched on and the connection with the instrumentation has been established, that is, before any irradiation intervention by the microdevice: this is the only occasion in which the 4-wire resistance measurement procedure necessarily takes place outside the irradiation phase, in order to analyze the temperature value of the tissue preliminarily and so evaluate a possible start of the infrared irradiation phase.

At any other time during the operation of the control system, the block of operations for measuring temperature will be carried out in conjunction with the irradiation phase of each loop cycle (precisely, during the final part of the communication phase with the 2635A SMU).

Indeed, as it is possible to deduce by observing figure 4.3.1, carrying out the temperature measurement procedure during the final part of the IR light supply phase allows obtaining values in °C that are much more accurate and reliable than at any other time at the internal of the i^{th} loop cycle, as the measurement is carried out on the flatter section of that curve, where the temperature assumed by the tissue can now be considered stationary. For this reason, the error of the temperature's measurement will be very low, practically negligible.

In order to make this possible, an inner while loop combined with the Matlab “pause” function has been introduced among the code instructions useful for setting the SMU appropriately by allowing the diode to be powered and therefore the irradiation by the optrode. This solution, as soon as the irradiation phase starts (driving current supply), make it possible to correctly count a time equal to:

$$phase\ ON - 1 [s]$$

Once this sort of “timer” implemented in Matlab expires, the temperature measurement procedure will start.

An indispensable and essential condition is to assume that the user will edit a feasible "phase ON" value by which the tissue can reach a stationary temperature value within 1 second before the end of the "ON" irradiation phase.

Considering that the measurement/acquisition time of the 5-resistances batch by the multimeter lasts almost 204 ms, starting the measurement block 1 second before the end of the irradiation phase is an acceptable choice as, except for any delays caused by machines, there would still be about $1 - 0.204 = 0.8 = 800$ ms of a margin between the end of the measurement phase and the end of the irradiation phase, for each cycle performed by the system.

4.5 Exposure time's counting method

A sufficient and necessary condition for the closed-loop control to stop irradiating (or even to definitely stop the instrumentation communication) autonomously, without the external intervention of the user, is to reach (or exceed) the maximum exposure time of the tissue at the target temperature set, via the GUI, during the control system initialization. Since the concept of "maximum time" is equivalent to that of "maximum number of consecutive loop cycles" during which the tissue is kept locally, thanks to the action of the optrode, at the target temperature, the software uses a time counter normalized with respect to the duration of a loop cycle in full operation by the optrode, namely the phase "ON" of the IR diode's supply current waveform.

Since the purpose of the time counter is to prevent tissue overheating due to excessive irradiation of the tissue as it is excessively exposed to a specific temperature, this value (appropriately updated after each useful cycle) must be able to be continuously compared to a reference value, in order to be able to verify the extent of this continuous exposure. This reference value is 95% of the maximum exposure time set via GUI by the user; obviously, this value is also normalized with respect to the theoretical duration of a single loop cycle, with the purpose of being systematically compared with the value assumed by the time counter.

$$T_{95\%} = \frac{0.95 \cdot Time\ max}{Phase\ ON}$$

For the closed-loop control to stop IR irradiation, it will be sufficient to reach the following condition:

$$Time\ counter \geq T_{95\%}$$

" $T_{95\%}$ " was introduced in order to place oneself in conditions of more excellent safety concerning overheating phenomenon prevention: it will be enough to reach at least 95% of the maximum time of exposure for the entire system to deactivate itself (end of communication with the instrumentation) or at least temporarily deactivate the optrode's irradiation, at the end of the current control cycle. How this reference value becomes a part of algorithm dynamics is explained in figure 4.5.1.

Once the comparison with this reference value satisfies the condition for which the maximum exposure time has been reached or exceeded, the control system may encounter two different situations:

- if the target temperature exceeds 40 °C, that is the threshold temperature beyond which first cerebral discomforts from thermal stress occur[7], the software will interpret this situation as a stop condition such that the system must automatically terminate the communication with driven instrumentation;
- if the target temperature set has a value within 40 °C, the system will force communication with the SMU by “providing” a supply current of 0 mA, allowing the system (net) to perform only temperature measurements. When the temperature value assumed by the tissue will be considered such that the IR irradiation must be restored, the time counter will be reset, which will then be ready for a new possible achievement of the target temperature within the same lifetime of the CLC system.

The system also takes into account an exceptional case: in the extraordinary case in which the set target temperature coincides with the starting temperature of the tissue, therefore without previous illumination phenomena, the system will limit itself only to carrying out temperature measurements (so that the software communicates only with 2100MM multimeter).

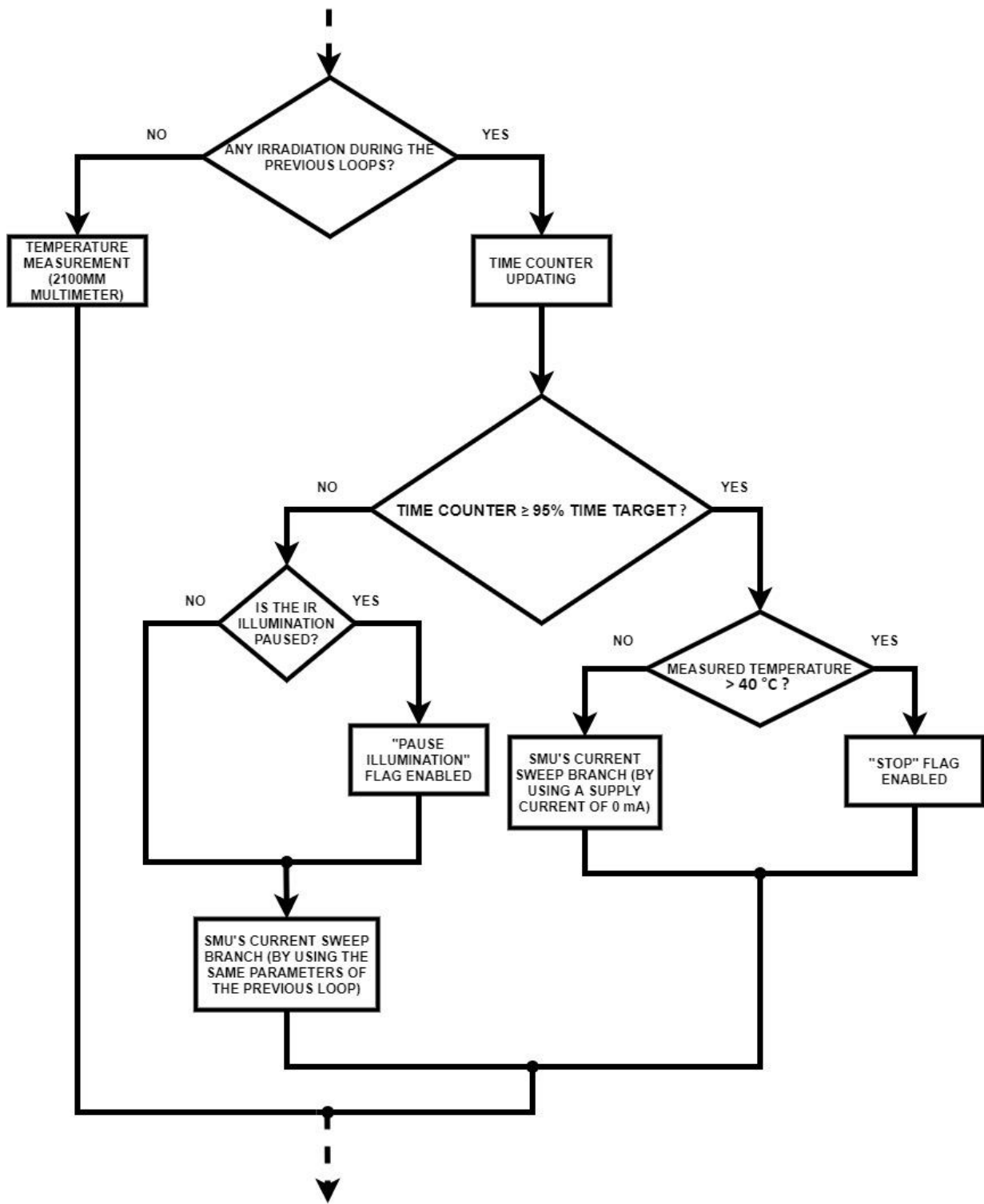


Figure 4.5.1 "Target reached" branch. Flowchart indicating the program branch in which the target temperature has been reached, so time counter starts to be updated.

4.6 Temperature error calculation and the accuracy's role

The temperature value, thus indirectly measured by the optrode, is then used to evaluate the ΔT error in relation to the user-edited target temperature value T_{TARGET} .

During each loop cycle, ΔT is calculated as follows:

$$\Delta T = T_{TARGET} - T_{MEAN}$$

As can be seen in figure 4.2.1, the value assumed by this error is decisive for the next step that the software will have to implement.

Theoretically, for the control system to fall into the right branch, the following cases should be considered:

- if $\Delta T > 0$ means that the T_{TARGET} has not yet been reached, which is why we fall back into the "Target not reached" branch, represented in figure 4.3.3;
- if $\Delta T < 0$ it means that the local temperature has exceeded the T_{TARGET} , which is why the system, according to the T_{TARGET} value despite the 40 °C threshold, is placed in the "illumination paused" or even in the "stop" condition (therefore exiting the control loop at the end of the current cycle);
- if $\Delta T = 0$ the perceived local temperature has reached the T_{TARGET} and one falls back into the "Target reached" branch, represented in figure 4.5.1, with possible consequent updating and control on the exposure time counter.

However, it should be noted that the temperature value measured by the optrode is strictly linked to the accuracy of the 2100MM multimeter, during the 4-wire Pt resistance measurements (as anticipated in paragraph 3.2). Hence, the ΔT calculated in this phase will also be affected by uncertainty:

$$\Delta T = T_{TARGET} - T_{MEAN}$$

$$\delta_{\Delta T} = \delta_{T_{TARGET}} + \delta_{T_{MEAN}} = \delta_{T_{MEAN}} = \delta_T$$

with $\delta_{T_{TARGET}} = 0$ since the T_{TARGET} is a constant value not affected by uncertainty, which is why its absolute accuracy is null.

The calculation of the ΔT error would be described as a whole:

$$\Delta T \pm \delta_{\Delta T} = T_{TARGET} - (T_{MEAN} \pm \delta_{T_{MEAN}})$$

When evaluating the value assumed by ΔT , the conditions for which the control system must perform a response operation rather than another are so modified:

- if $\Delta T > +\delta T$ the system falls into the "Target not reached" branch;
- if $\Delta T < -\delta T$ the irradiation will be temporarily paused if T_{TARGET} is lower than 40°C [7] (threshold temperature), otherwise the communication with the instrumentation will be interrupted at the end of the current cycle, due to the unquestionable and concurrent overcoming of the T_{TARGET} the threshold temperature;
- if $-\delta T \leq \Delta T \leq +\delta T$ the system falls into the "Target reached" branch;

The calculation process of this accuracy is carried out, in the manner described below, during each loop cycle.

The batch of five measured resistances:

$$R_X = \{R_1 R_2 R_3 R_4 R_5\}$$

X^{th} resistance value measured by the multimeter[25]:

$$R_X \pm \text{absolute accuracy} = R_X \pm \delta_{R_X}$$

$$R_X \pm (\% \text{ of reading} + \% \text{ of range})$$

$$R_X \pm (0.015\% R_X + 0.002\% 1 \text{ k}\Omega)$$

with $X = 1, 2, 3, 4, 5$.

$$R_{TOT} = R_1 + R_2 + R_3 + R_4 + R_5$$

We now proceed with the calculation of the R_{TOT} relative accuracy:

$$\begin{aligned} \varepsilon_{R_{TOT}} &= \varepsilon_{(R_1+R_2+R_3+R_4+R_5)} = \\ &= \frac{\delta_{(R_1+R_2+R_3+R_4+R_5)}}{R_1 + R_2 + R_3 + R_4 + R_5} = \\ &= \frac{\delta_{R_1} + \delta_{R_2} + \delta_{R_3} + \delta_{R_4} + \delta_{R_5}}{R_{TOT}} \end{aligned}$$

The average resistance value and its relative accuracies are calculated:

$$R_{MEAN} = \frac{R_1 + R_2 + R_3 + R_4 + R_5}{5} = \frac{R_{TOT}}{5}$$

$$\varepsilon_{R_{MEAN}} = \varepsilon_{R_{TOT}} + \varepsilon_{DENOMINATOR} = \varepsilon_{R_{TOT}}$$

The R_{MEAN} absolute accuracy is then calculated:

$$\delta_{R_{MEAN}} = \varepsilon_{R_{TOT}} \cdot R_{MEAN} = \frac{R_{MEAN}}{R_{TOT}} \cdot (\delta_{R_1} + \delta_{R_2} + \delta_{R_3} + \delta_{R_4} + \delta_{R_5})$$

At this point, the Callendar-Van Dusen equation is used:

$$\begin{aligned} R_{MEAN} &= R_0(1 + \alpha T) \\ T &= \frac{R_{MEAN} - R_0}{R_0 \alpha} = T_{MEAN} \\ \varepsilon_T &= \varepsilon_{(R_{MEAN} - R_0)} + \varepsilon_{(R_0 \alpha)} = \\ &= \frac{\delta_{(R_{MEAN} - R_0)}}{R_{MEAN} - R_0} + \varepsilon_{R_0} + \varepsilon_{\alpha} = \\ &= \frac{\delta_{R_{MEAN}} + \delta_{R_0}}{R_{MEAN} - R_0} = \frac{\delta_{R_{MEAN}}}{R_{MEAN} - R_0} = \varepsilon_{T_{MEAN}} \\ \delta_{T_{MEAN}} &= \delta_T = \frac{\delta_{R_{MEAN}}}{R_{MEAN} - R_0} \cdot T_{MEAN} \end{aligned}$$

It can be seen that R_0 and α accuracies were considered negligible.

The complete temperature measurement will then be explained as

$$T_{MEAN} \pm \delta_{T_{MEAN}} = T_{MEAN} \pm \delta_T$$

Finally, δ_T is expressed as a function of all known terms:

$$\begin{aligned} \delta_T &= \frac{\delta_{R_{MEAN}}}{R_{MEAN} - R_0} \cdot T_{MEAN} = \\ &= \frac{\varepsilon_{R_{TOT}} \cdot R_{MEAN}}{R_{MEAN} - R_0} \cdot T_{MEAN} = \\ &= \frac{R_{MEAN}}{R_{TOT}} \cdot (\delta_{R_1} + \delta_{R_2} + \delta_{R_3} + \delta_{R_4} + \delta_{R_5}) \cdot \frac{T_{MEAN}}{R_{MEAN} - R_0} = \\ &= [5 \cdot (2000 \cdot 10^{-5}) + R_{TOT} \cdot 15 \cdot 10^{-5}] \cdot \frac{R_{MEAN} \cdot T_{MEAN}}{R_{TOT}(R_{MEAN} - R_0)} \end{aligned}$$

4.7 The end of the closed-loop control

The "stop" condition detected by the system, within a loop cycle, which can occur automatically (utilizing an appropriate "STOP" flag activation) or manually, can be achieved in several ways:

- automatically, caused by incompatibility between the values of maximum exposure time and waveform's phase ON of the IR diode's supply current, both set by the user;
- automatically, due to reaching or exceeding the maximum exposure time (if the target temperature exceeds 40 °C);
- automatically, assuming target temperature higher than the 40 °C threshold, due to the overcoming the limit value for the local tissue temperature (overheating);
- automatically, due to exceeding the maximum value of the diode's supply current;
- manually, in case the user has pressed the "START & STOP" toggle button from the GUI while system working.

The control system exits the loop at the end of the current loop cycle. Once this happens, for the last time, five more measurements and acquisitions of the Pt integrated sensor's resistance value are carried out and appropriately written on file. This operation is performed in order to evaluate, during the system validation phase, the actual acquisition duration of a single batch of five measurements and therefore, the deviation from the theoretical value used in the design calculations.

Finally, the communication with both the multimeter and the SMU is permanently closed; the buffers and variables used for the last performed acquisition cycle are also cleaned for the last time.

Now that the dynamics of the designed software have been described in detail, the presentation regarding the testing phase of the system is reported.

5 Validation

In order to test the designed CLC system, a protocol has been created, whose steps are listed in the following paragraphs of this chapter. This protocol has the purpose of demonstrating the correct functioning of the software under the different and possible operating conditions in which the system mentioned above may encounter.

2 ml of tap water were used in a polyethylene cylinder, to carry out the various in vitro tests described below, since water is the closest candidate compared to an in vitro sample of brain tissue for the average percentage of water contained in the latter.

The optrode used for the validation phase was the "OT1".

The room temperature of the laboratory where the tests were carried out was approximately 23 °C and 24 °C.

It is necessary to specify that, for the sole purpose of successful testing, the in vitro setup and the technical operating limits of the diode require, in most of the tests carried out, the lowering of the threshold temperature (that is, at the level of code, the perceived temperature beyond which the system, if particular conditions are met, can autonomously terminate the communication with the connected instrumentation) from 40 °C to 24.55 °C. This adjustment is due to the starting room temperature and because the in vitro medium used is different from that for which the design calculations described in the previous chapters were carried out: the current calculations made based on data relating to the cerebral cortex are such as to give rise to thermal jumps approximately between 0.3 °C and 0.4 °C instead of 0.5 °C.

The various validation tests are then presented below.

5.1 System behaviour in regular operation

Figure 5.1.1 below shows how the software and the setup with which it communicates respond well to the input parameters under normal operating conditions.

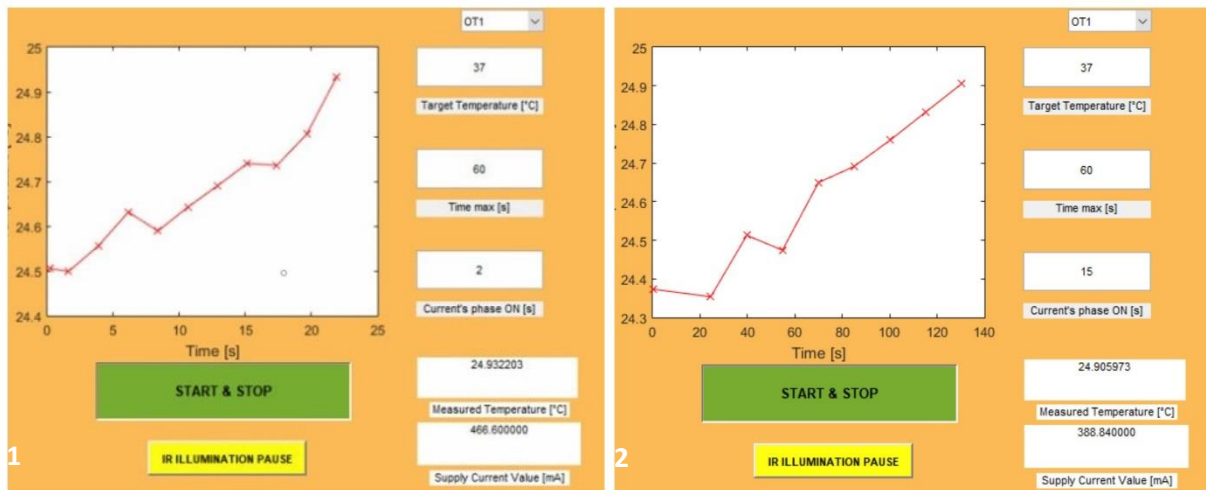


Figure 5.1.1 Control system's GUI in regular operation conditions. (1) “Target Temperature” = 37 °C, “Time max” = 60 s, “Current's phase ON” = 2 s. (2) “Target Temperature” = 37 °C, “Time max” = 60 s, “Current's phase ON” = 15 s.

In particular, it can be noticed how the inter-samples distance is attributable, observing the time axis, to the edited current's phase ON value.

Indeed, as the current's phase ON decreases, it is possible to appreciate more the measurement limits of the 2100MM multimeter, with a greater probability of noticing the negative slopes of the plotted curve during operation. This behaviour is justified by the fact that, with a shorter inter-samples distance, any random temperature oscillations of the irradiated sample are more easily observed.

5.2 Inappropriate set maximum exposure time demonstration

This test was performed solely to demonstrate the ability of the software to report a “Time max” value incompatible with the declared supply current's phase ON. As shown in figure 5.2.1, the selected input values ("Time max" = 5 s and "Current's phase ON" = 30 s) determine the appearance of an error message from the system, which will carry out the acquisition of a single batch of 5 resistance measurements in order to communicate the measurement/acquisition duration of that batch.

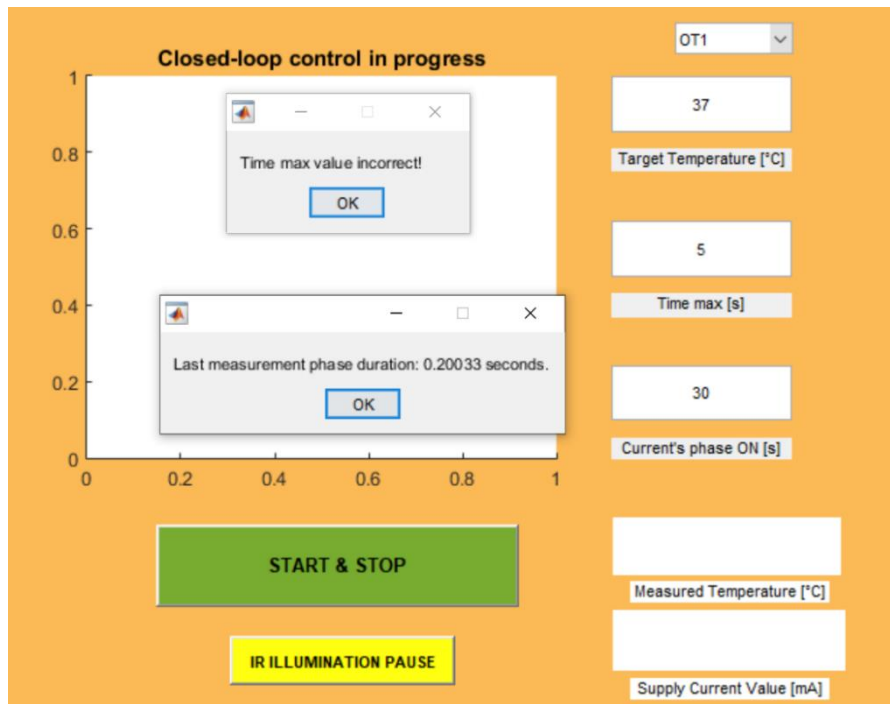


Figure 5.2.1 Incorrect “Time max” value demonstration.

5.3 Maximum working diode current exceeding demonstration

Figure 5.3.1 represents a classic case in which, based on the input parameters passed to the system, the CLC system stops communicating with the connected instrumentation due to exceeding the 490 mA set as the upper limit for the working supply diode current. In fact, observing this figure, it is possible to notice how the target temperature set is too high and difficult to reach due to the starting temperature of the tap water (just below 24 °C, in this example) and considering that, during each loop cycle, a ΔI of current has added to the current supplied to the diode in the previous cycle. In this case, it is noted that, once the tap water reaches a temperature of 24.65 °C, the corresponding current value supplied to the diode ensures that the system automatically recognizes the condition for which the system control must stop its regular operation, just communicating to the user the acquisition duration of the last batch of resistance values through the appropriate message box.

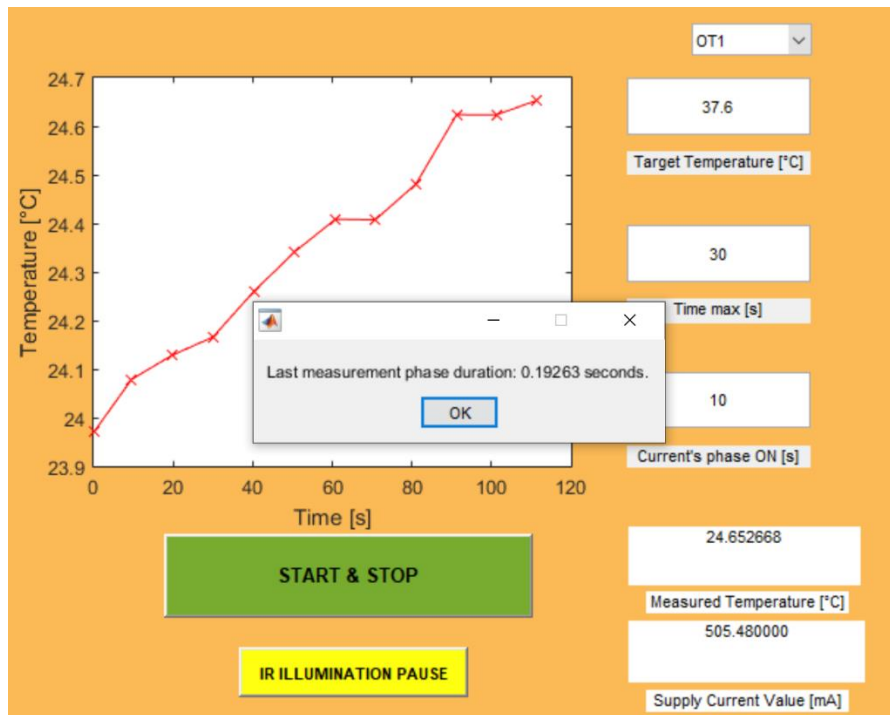


Figure 5.3.1 Maximum working diode current exceeding.

5.4 Set maximum exposure time validation

During the test described below, the ability of the CLC system to autonomously terminate its control operations was demonstrated, if the maximum exposure time at a target temperature which is higher than the threshold set by code (which is recalled having been brought, in this experimental phase, to a value of 24.55 °C) has been reached and therefore exceeded.

As can be seen in figure 5.4.1, the input parameters set passed to the system is characterized by the following values:

- “Target Temperature” = 24.8 °C;
- Maximum time of exposure at the target temperature = 30 s;
- Supply current's phase ON = 10 s.

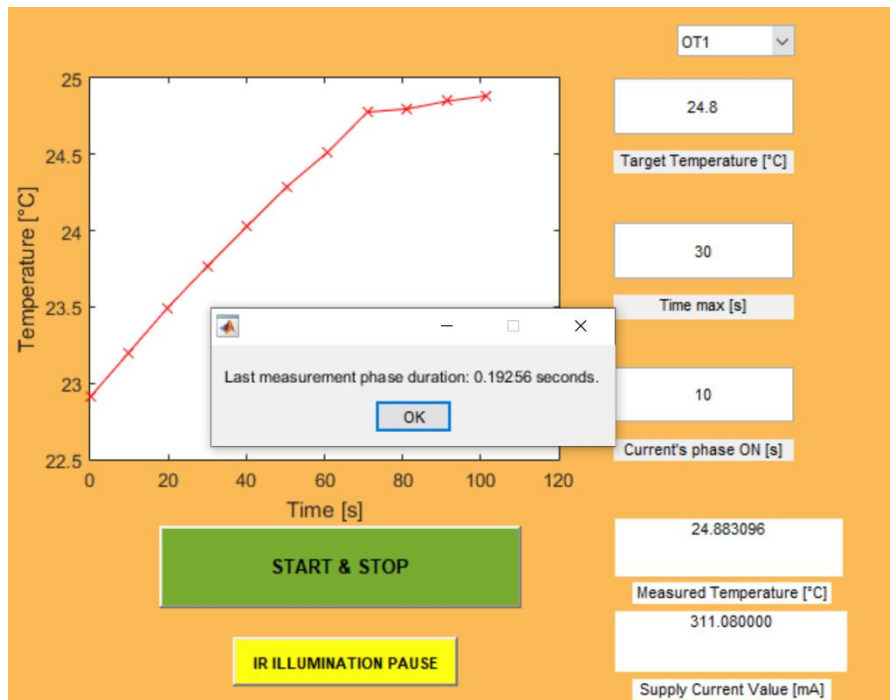


Figure 5.4.1 Maximum exposure time validation.

The figure above shows how the section of the graph corresponding to the last four samples of measured temperature assumes an almost stationary trend on the GUI plot. This behaviour demonstrates that the last four samples measured are such that the value $\Delta T = T_{\text{TARGET}} - T_{\text{MEAN}}$ falls within the $\pm\delta_T$ acceptance range which, in other words, indirectly informs the user of how the target temperature can be considered reached. This condition, from the moment in which this target has been reached and as explained in paragraph 4.5, determines the updating of a time counter in conjunction with the irradiation of the in vitro sample at the same optical power (and therefore the same supply current delivery to the diode) used during the immediately preceding loop cycle. The table below shows the ΔT values relating to the last five measured temperature samples observable in figure 5.4.1, certifying how, compared to the corresponding accuracy values calculated by the software, the optrode maintains the same optical irradiation power during the last three loop cycles (each of which lasting approximately 10 s, correctly obtaining a maximum exposure time at the target temperature of about 30 s).

# sample	ΔT (°C)	δT accuracy (°C)
i	-0,08	0,08137
i - 1	-0,05	0,08136
i - 2	0	0,08135
i - 3	0,02	0,08135
i - 4	0,29	0,08131

Table 5.4.1 ΔT and accuracy values of the last five measured temperature values observed in figure 5.4.1. With i = last measured temperature sample before the end of the CLC system operations.

By observing the table, it can be seen that during the experiment represented in figure 5.4.1, the temperature sample "i - 4" was the last value to consider the temperature assumed at that moment by the tap water out of the $\pm \delta T$ acceptance range. The samples that go from "i - 3" to "i" are relative to the "Target reached" branch case.

Finally, it can be noticed how the accuracy value assumed in the various loop cycles always fluctuates slightly around the same average value, since the appreciable temperature variations in the various cycles during these validation experiments are minimal.

5.5 Evaluation of the resistance batches acquisition duration

This phase of the validation was performed with the simple purpose of evaluating the deviation of the actual measurement/acquisition duration of a single batch of resistance measurements compared to the theoretical assumed value. The algorithm was launched five times, and the content of the message box that the user can view once the system is at the end of its operation was evaluated.

The estimated durations, expressed below in milliseconds, each relating to a single batch are then evaluated on five different trials, as can be seen schematically in the histogram of figure 5.5.1.

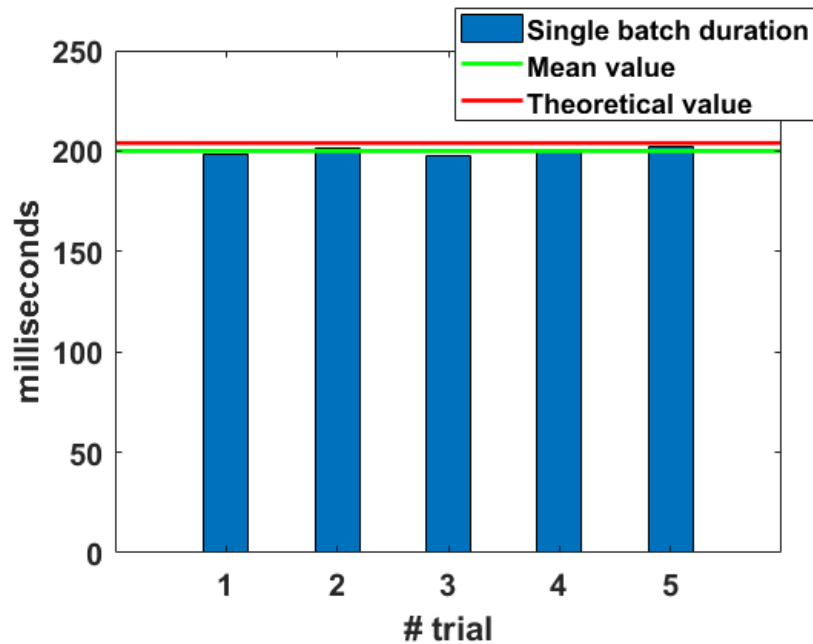


Figure 5.5.1 Duration of the last batch's measurement/acquisition on five algorithm's launch trials.

The average value of the five values represented in the histogram is equal to **200.02 ms**, with therefore an acceptable deviation of **1.95 %** compared to the theoretical value previously declared and equal to **204 ms**.

5.6 Recommended “Phase ON” values range for the user

This test has been performed in order to suggest a range of values that can guide the user towards an appropriate choice of the high phase of the supply current waveform, thus guaranteeing the proper functioning of the entire system.

Four trials were performed during each of which a different “Current’s phase ON” value was tested, evaluating the feedback of the CLC system to this input parameter.

It is also specified that, contrary to what was stated in the introduction of this chapter and in order to qualitatively and effectively describe the following test, the threshold at the algorithm level has been temporarily restored to its original value of 40 °C.

- **Phase ON = 2 s**

For this first trial, a target temperature of 24.8 °C and a maximum exposure time of 20 s have been used. The outcome is shown in the following figure 5.6.1.

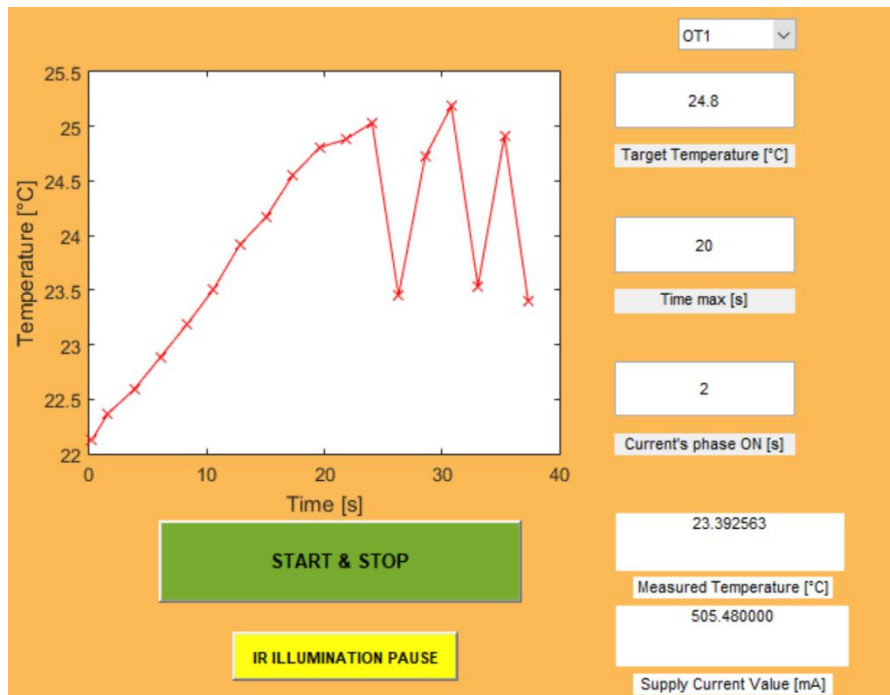


Figure 5.6.1 “Phase ON” = 2 s trial.

The shape assumed by the GUI graph presents ripples due to the repeated suspension and restoration of the lighting by the optrode, due to the sudden exceeding of a target temperature lower than the threshold set at 40 °C.

The use limit of a too-short high phase duration of the current waveform can be found, in this example, around 25 °C. In fact, during its gradual increase in temperature due to the action of the optrode, the tap water sample reaches a temperature such that the relative ΔT error is correctly within the acceptance range $\pm\delta_T$, just before 20 s since the CLC system has been powered ON, has elapsed. It is easy to see, however, that the "Time max" value imposed by the user has not been respected, as although the target temperature is reached, the SMU provides the laser diode with a further ΔI of current, thus bringing the temperature of the tap water out of the acceptance range and thus triggering the phenomenon of ripples observable in the figure above. The anomalous behaviour observed, in the live plot, around 25 °C could have been caused by an incompatibility of the execution speed of the SMU despite the sequential code lines of the Matlab algorithm, probably related to a too low duration of the current's waveform phase ON and therefore of the single loop cycle. This phenomenon may not have allowed the instrumentation to adapt in time to changes in the conditions of the software in

the various execution branches. Further investigations will have to be carried out in the future in order to clarify the specific case described above definitively.

- **Phase ON = 5 s**

For the subsequent trial and the next, a “Target Temperature” of 24.48 °C and an exposure “Time max” of 20 s were used as input parameters. For example, the result represented in figure 5.6.2 can be observed:

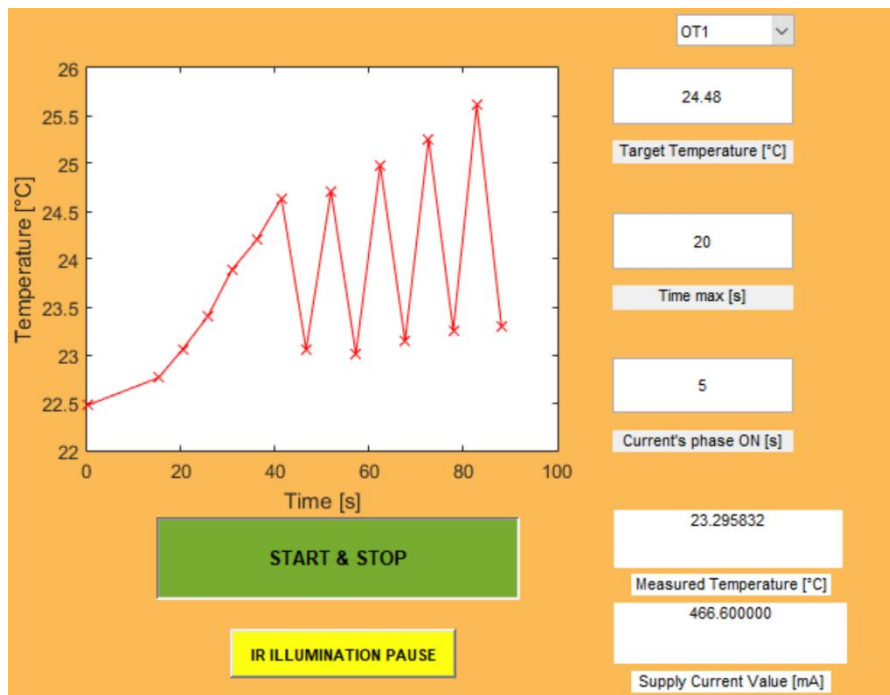


Figure 5.6.2 “Phase ON” = 5 s trial.

It is useful to point out that in this trial (and in the following one) the temperature level assumed by the tap water has never been such that the ΔT error could correctly fall within the acceptance range $\pm\delta_T$. This phenomenon may occur due to the design calculations inherent in the choice of the ΔI current value useful to induce thermal jumps on the irradiated target have been designed for nervous tissue samples and not for water. Further investigations related to the CLC system's application to tissue samples will be done in order to assess the just described situation.

It can be said that, contrary to the anomalous behaviour of the previous trial, the measured temperature value is always and correctly interpreted by the system as "out of the acceptance range": depending on the situation in which the system encounters, it provides tissue irradiations or pauses the lighting depending on whether the algorithm follows the “Target not reached” branch or the “Target exceeded” branch.

- **Phase ON = 15 s**

The starting conditions of this trial are the same as the previous one, as can be seen in figure 5.6.3:

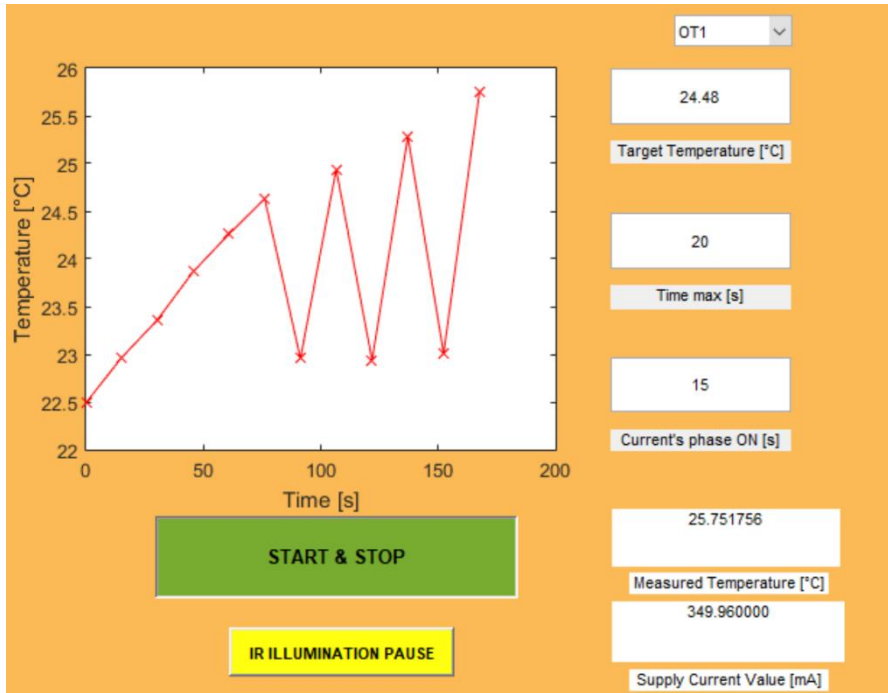


Figure 5.6.3 “Phase ON” = 15 s trial.

Even then, the different branch conditions have been correctly interpreted by the algorithm. By observing the ripples of the graph, it can be seen how the amplitude of each of them is always more significant as the operating cycles follow one another. This phenomenon is justified by the fact that every time the IR irradiation is temporarily disabled due to exceeding the edited target temperature, the last current value supplied by the SMU is kept in memory; once the conditions useful for restoring the lighting of the sample are met, a ΔI of current at the last saved supply current value is added, thus resulting in a thermal transient (and therefore a ripple) with an amplitude more significant than the previous one.

- **Phase ON = 60 s**

It has been chosen to opt for this trial, as values of target temperature and maximum time of exposure, respectively 24.48 °C and 90 s. More details are shown in figure 5.6.4:



Figure 5.6.4 “Phase ON” = 60 s trial.

This time it was decided to analyze through the GUI toolbar a close-up of the peak of the first ripple obtained, inferring that although the system recognizes and correctly interprets the branch conditions, a more extended phase ON further decreases the possibility of bringing the irradiated sample temperature in the acceptance range useful to consider the target temperature as correctly reached. The greater the distance between two measured temperature samples (as happened in this trial), the greater the intersample temperature jump, since the exposure time of the irradiated sample to a specific optical power increases in the same way.

In the light of these tests carried out, the actual recommended range for the user that guarantees proper operation of the system and that at the same time allows a good compromise in terms of duration of exposure to specific optical output power is declared as follows:

$$5 \text{ s} \leq \textit{Recommended "Phase ON"} \leq 20 \text{ s}$$

5.7 Target temperature lower than room temperature test

The system behaviour if the set target temperature is lower than the room temperature has been investigated.

Figure 5.7.1 shows the results of a test in which the following test input parameters were used:

- “Target Temperature” = 20 °C;
- “Time max” = 30 s;
- “Current's phase ON” = 10 s.

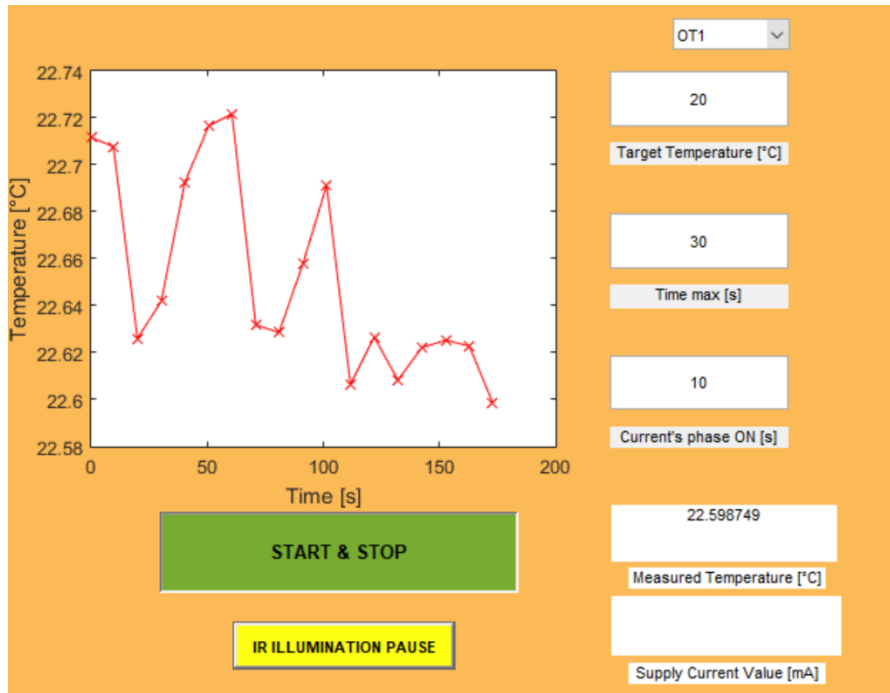


Figure 5.7.1 Target temperature lower than room temperature test.

The empty supply current’s live-updating box indicates that the laser diode is never (correctly) powered for the duration of the test. The distance between two samples of measured temperature is always about 10 s, as the system interprets this test condition in a similar way to the "target temperature exceeded" case. During each loop cycle, the PLC system correctly communicates with the SMU “by forcing” a supply current of 0 mA, making only the local temperature measurement net of each cycle. In other words, in the graph above, random changes in the tap water temperature have been appreciated.

In this particular case, the system can only be turned off manually by the user via GUI; otherwise, it would ideally continue to work indefinitely: this would happen because the prototype of this project was designed to increase the temperature of the tissue sample and is therefore not equipped, at the moment, of stop conditions for this particular situation.

5.8 IR illumination pause test

The system response to the possible use, by the user, of the button useful to pause the irradiation delivered by the optrode has been tested. Figure 5.8.1 proposes three different and consecutive moments, during the same test, in which this function is enabled and then disabled again.

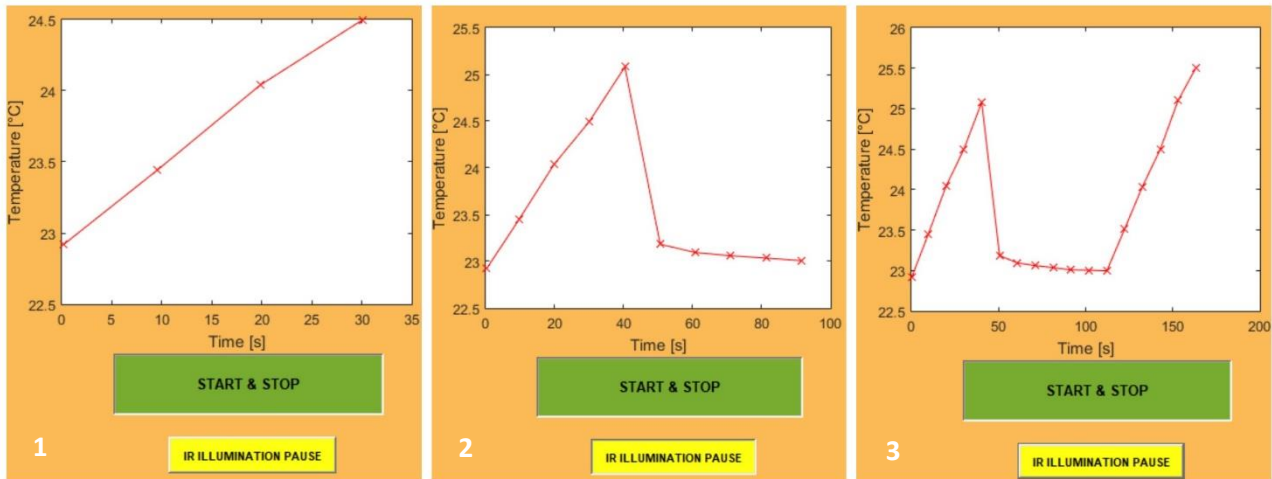


Figure 5.8.1 "IR Pause Illumination" button use. (1) Button disabled during the first about 30 s of testing. (2) Button enabled around 40 s since the test started. (3) Button disabled almost 50 s since the irradiation was paused.

It is possible to specify that although the lighting has been restored, looking at the x-axis of the graph, at the second n. 93 (i.e. in correspondence with the fifth sample observable in the plateau phase, due to the paused irradiation phenomenon, present in the third image of figure 5.8.1) it is possible to observe a new increase in the temperature of the irradiated sample only three cycles after the irradiation has been restored using the appropriate button. This behaviour is because, “by forcing” a supply current of 0 mA while the toggle button is enabled, this current value will also be the last one stored by the system: once this mode is disabled and the system needs to irradiate the sample again, a ΔI of current will be added to the overall supply current which, in this case, will assume a lower value than the datasheet's $I_{\text{threshold}}$ for the next two loop cycles; this transitory and momentary condition will have the sole effect of not causing any thermal jump until the $I_{\text{threshold}}$ is again exceeded.

5.9 Live “Target Temperature” editing

During the execution of this test, the possibility for the system to adapt to changes in the target temperature value, during the succession of its operating cycles, it has been demonstrated.

This test is summarized in figure 5.9.1 below, using a supply current phase ON of 10 s and a maximum exposure time of 30 s. The three “Target Temperature” values tested and consecutively communicated to the system during its operation are respectively **23.5 °C**, **24.5 °C** and **25.5 °C**.

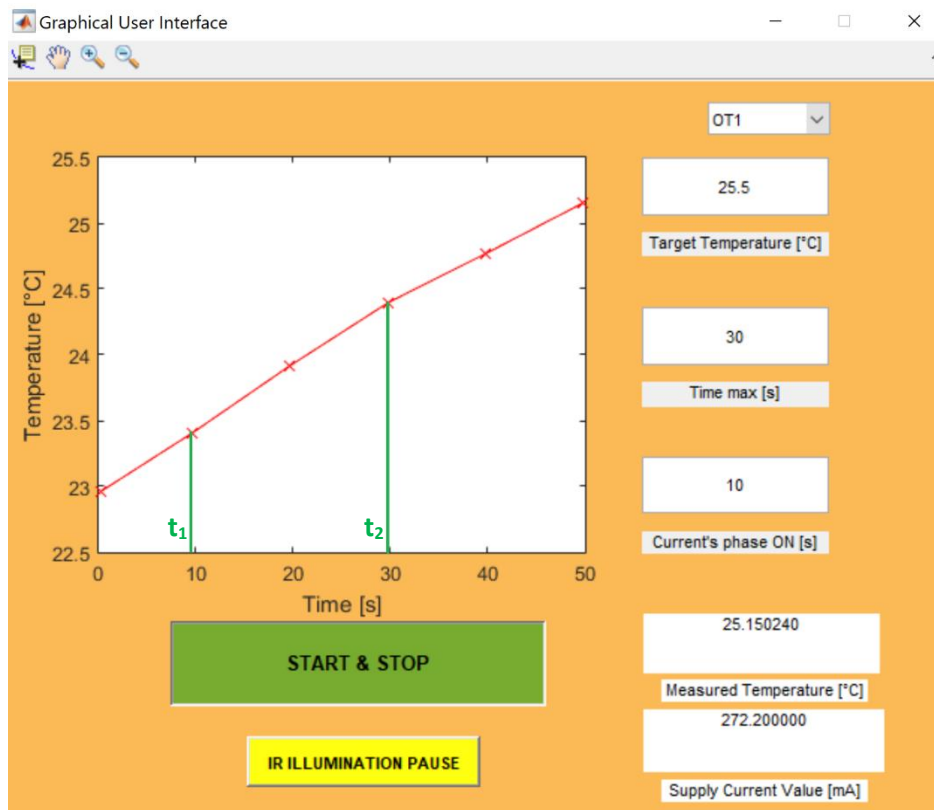


Figure 5.9.1 “Target Temperature” value live editing test.

The time points marked in green on the figure above indicate the moments in which, during the test, it was decided to change the “Target Temperature” value to check the system feedback:

- t_1 = precisely 9.64 s from the start of the test, “Target Temperature” value has been changed from 23.5 °C to 24.5 °C;
- t_2 = precisely 29.76 s from the start of the test, “Target Temperature” value has been changed from 24.5 °C to 25.5 °C.

It is easy to understand how the system correctly adapts, during its operation, to the changes made in real-time by the user. In fact, it was decided to proceed in such a way that the software found the "Target not reached" condition for the entire duration of the test.

5.10 Live supply current phase ON editing

Similarly, as the last validation test presented in this thesis, the possibility of modifying the supply current waveform's phase ON during the operating cycles of the system has been demonstrated. Figure 5.10.1 shows how this input value is modified from 15 s to 5 s during regular operation of the CLC system. For this test, the algorithm threshold was reset to 40 °C.

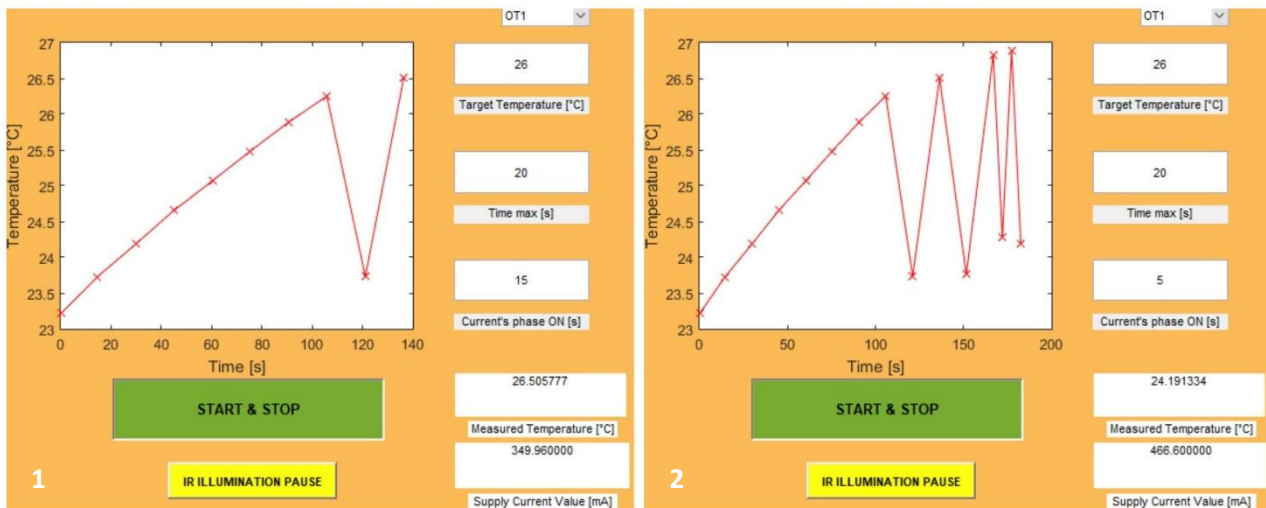


Figure 5.10.1 “Phase ON” value live editing test. (1) System switched on using a “Phase ON” of 15 s. (2) “Phase ON” value changed to 5 s during the normal system's functioning (almost before 150 s since the system started working). “Target Temperature” = 26 °C; “Time max” = 20 s.

It is easy to observe how the peak-to-peak amplitude of the ripples increases as the supply current's phase ON increases. This phenomenon is because when the lighting is (temporarily) suspended, the longer the phase ON communicated to the system is, the longer the time allowed to the irradiated sample will be to cool-down, letting it to reach lower temperatures while getting cold, before the irradiation by the optrode is restored. With shorter phase ON values, shorter cooling time is granted to the sample concerned, so that the peak-to-peak amplitudes of the relative ripples are indeed smaller.

6 Potential applications and benefits

As previously mentioned, over the years, brain thermorecording has not been a priority object at the research level and is a subject in continuous evolution and deepening.

The first in vivo results obtained in the laboratory, before this thesis work, using optrodes, turned out to be quite useful and promising. Nevertheless, to get more detailed knowledge about the effect of IR irradiation or local temperature increase on local neural activity, the developed control system would be, for Hungarian brain researchers, a useful tool since it will provide self-adjusting temperature control. In fact, without a control system of this type, only IR diode's supply current is adjustable, making the experimental phase more vulnerable to phenomena such as light source ageing, which determines weaker emission with similar set current values.

A self-adjusting parameters tool can help the experimental phase to intervene in these possible situations without compromising the results, considerably attenuating these types of source of errors.

Main potential applications of the developed system could concern studies of clearer thresholds and limits of different neural modulation states, related to more accurate temperature levels.

Other possible and interesting uses of the CLC system could concern, for example:

- graphic monitoring of pathological hyperthermia phenomena and simultaneous evaluation of the electrical activity, during in vivo tests and without the need for stimulation, of epileptic or TBI subjects;
- pathological hyperthermia phenomena simulation, locally;
- graphic monitoring of the local temperature trend to evaluate the role of the temperature in cerebral homeostasis;
- high temperature-induced stress tests on the intra-sample and inter-samples variability of neural tissue concerning the morphological and functional response of neuronal populations at positive temperature gradients;
- in-depth in vitro and in vivo testing, by crossing the use of this tool with other types of tests, to better evaluate the optical output powers suitable to trigger the increase (firing) or decrease (suppression) of the electrical neuronal activity in various areas of the brain;

- study of thermal blocking of neuronal APs (Action Potentials) propagations on myelinated and unmyelinated nerves;
- in-depth evaluation of the levels of optical power, temperature and supply current useful to activate, through the CLC system, predetermined cortical areas during in vivo experiments;
- in vivo testing concerning possible IR applications for therapeutic purposes.

It is sure as many limits found in the prototype validation phase will be fixed in order to make the system more and more accurate and performing.

Making the “Current's phase ON” values range wider for the user is undoubtedly a feature to improve, in order to provide a broader range of usable values and thus allowing more variable experiments, from this point of view. Among the other possible improvements, there is certainly the possibility of making the system more "patient" to the maximum diode's working current, thus allowing the optrode, in some instances, to provide higher thermal transients without the instant suspension of the system control (which currently occurs as soon as the detected and delivered supply current matches the relative datasheet's maximum value). This modification should, however, be implemented by finding a compromise with the diode damages avoidance. It would also be useful to clarify the alleged discrepancy, mentioned in paragraph 5.6, between the sequential action speed of the Matlab software's code lines and the SMU response speed, in the case in which shorter current waveform's phases ON are used.

Once the CLC system is used for brain tissue samples tests, it will undoubtedly be necessary to evaluate its behaviour in certain situations. For example, the actual value in °C of the thermal difference between two consecutive measured samples of temperature will be evaluated, during the operation at irradiation regime by the optrode connected to the control system, comparing this value with the theoretical values declared in the project calculations of this thesis work. The actual reliability of the wideness assumed by the $\pm \delta_T$ acceptance range will be tested, possibly taking into consideration new ways that would lead to opting for more comprehensive and broader acceptance ranges (for example, choosing to consider the accuracies of R_0 and α as non-negligible, during the previously mentioned calculation). It will also be necessary to evaluate the expected increase in the number of measured temperature values correctly recognized in the calculated acceptance range, thus making the maximum time of exposure value edited by the user more usable.

7 Conclusions

The current state of the art regarding brain thermorecording, as well as in-depth knowledge of the role and dynamics involving temperature in the brain, still have considerable margins for improvement.

The brain is undoubtedly one of the most sensitive organs to temperature changes. It can answer both in terms of morphological variation of its structures and from a functional point of view in the case, for example, of phenomena of evoked stimulation or inhibition of neuronal electrical activity. These can be respectively caused by controlled space-time thermal gradients and by external irradiation proportional to the baseline temperature of the concerned district. At the basis of the influence of the excitability of the nervous network by temperature changes, lies the role of thermally active receptors TRP at the level of synaptic transmissions.

A Matlab-based closed-loop control system (CLC) has been developed, with the collaboration of the Research Group of Implantable Microsystems, Pázmány Péter Catholic University and Hungarian Academy of Sciences, as a support tool for brain researchers during *in vitro* and *in vivo* infrared neural stimulation experiments.

As per the definition for a feedback-based control system, a CLC system adjusts its operating parameters in order to minimize the errors of its outcome to a reference value. A system of this kind which, moreover, takes into account the previous history of its outcome, acts proportionally to the calculated error and the frequency of variation of the measurements makes itself a PID system. While making an analogy with the project presented in this thesis, the system described here provides for the self-regulation of the infrared optical power delivered locally by a MEMS technology-based implantable microdevice called optrode, designed to be implanted in deep brain tissue. By exploiting the multifunctionality of this microdevice, consisting in particular in being able to both deliver infrared light from its tip and provide temperature measurements thanks to the presence at the optrode's shaft of an embedded resistive Pt filament (as an RTD), the designed tool can ensure that the irradiated tissue reaches the desired temperature by the user, in a controlled and safe manner.

The proposed system is composed of software which communicates with electronic instrumentation, consisting of a multimeter and a Source-measure Unit (SMU). Based on the resistance measurements of the optrode's Pt filament, carried out by the multimeter in 4-wire mode, suitably converted into the

relative temperature value (expressed in °C) utilizing the Callendar-Van Dusen relationship, the software modulates, during each operating loop cycle, the current delivered by the SMU to power an IR laser diode. This last component, coupled to multimode optical fibre, in turn optically coupled to the Si integrated waveguide etched in the optrode chip's backbone, determines the delivery of infrared light from the optrode's tip and therefore the induction of a thermal transient locally to the stimulation area affected.

The developed software includes a Graphical User Interface (GUI) to allow the user to enter inputs such as one of three sets of sensor coefficients (TCR and R_0) relating to three different optrodes that can be integrated with the CLC system, save in ".csv" format the resistance values measured and acquired during system operation, the target temperature (in °C) that the irradiated tissue must reach, the maximum exposure time (in s) of the tissue at the target temperature set as input (precisely the 95% of this value for further reasons of tissue overheating prevention) and the duration (always in s) of the ON phase of the supply current waveform, equivalent to the average duration of an operating loop cycle and therefore to the continuous stimulation of the tissue at a specific optical power. Furthermore the user, in addition to being able to view in real-time the trend of the local temperature taken by the irradiated sample, also has the possibility of pausing the irradiation carried out by the optrode or arbitrarily terminating, at any time and permanently, the communication of the software with the instrumentation with which it interfaces. If the measured local temperature is identified as higher than that whose value has been entered via the GUI or the maximum exposure time has been reached or exceeded, the system can temporarily and autonomously interrupt the irradiation via optrode, in waiting for the tissue sample cool down, however, if the temperatures involved are below a predetermined threshold of 40 °C (reference temperature from which the first discomforts due to cerebral thermal stress could occur). Under the same conditions found but at temperatures higher than the threshold mentioned above, the system definitively interrupts the operational flow of the system.

Before implementing the CLC system, specific quantities such as the absolute optical power exiting the probe tip and the waveguiding efficiency of the passive embedded infrared waveguide of the probe are measured with particular instrumentation.

Starting from a value of 77.8 mA as diode supply current delivered by the SMU, which value would determine a first thermal jump of about 1 °C, during every consequent iteration, a further ΔI of 38.88 mA is provided in order to let the irradiated tissue achieve, in a gradual way, the target temperature edited by the user. This current supplement guarantees a theoretical thermal jump between two measured temperature samples of about 0.5 °C, a value still considered sufficient to be able to appreciate functional alterations in the nervous system. These current values were calculated using

the available literature regarding the stimulation of the rats' neocortex, together with the datasheets of the instrumentation made available, also taking into account power losses phenomena at the level of light propagation in the optical fibre and the Si waveguide, without neglecting the possible ageing of the diode. The waveform of the used current is a square wave with a duty cycle of 100%,

The communication with the SMU, concerning parameters setting such as current values, current range and voltage compliance limit, has been obtained in LUA programming language. These LUA commands have been sent to SMU within the Matlab environment while implementing the whole software's code.

Regarding the approach used to perform temperature measurements via multimeter, specific parameters of the instrument are set via software when the system is switched on, such as the measurement range or A/D converter integration time. In order to obtain a temperature value with good precision, five resistance values are measured during each cycle, averaged to then obtain the relative and unique temperature value, with an acquisition duration of the batch containing the five measurements of approximately 204 ms. During each measurement cycle following the first, this procedure is carried out within 1 second of the end of the probe irradiation phase, to obtain the most precise temperature values possible, since achieved in correspondence of the flatter section of the irradiation-induced thermal transient of the observed sample.

During the cyclical evaluation of the error ΔT between the measured temperature and the target temperature in order to deliver or not the infrared light on the sample, an acceptance range has been introduced equal, in terms of absolute amplitude, to double the uncertainty of the multimeter linked to the measurement, so that it can help the system to avoid errors of interpretation due precisely to the accuracy of the measuring instrument.

The validation of the CLC system was carried out in the laboratory, with a room temperature between 23 and 24 °C, using as irradiated sample 2 ml of tap water, considered the candidate closest to the nervous tissue by the percentage of water content to its internal. The validation tests were carried out with a single optrode. It was necessary, in some cases, to modify the threshold temperature declared in the software from 40 °C to 24.55 °C, due to the room temperature level compared to the human body's baseline temperature and to the nature of the sample to be irradiated, used in this part of the project. The main operating situations of the system were presented and demonstrated, highlighting any limitations of the prototype that will be subject to improvements later. The system was shown in normal operating conditions. The ability to evaluate the possible inadequacy of specific input parameters or the exceeding of thresholds such as that of the maximum working diode current useful

for safeguarding the IR laser diode was demonstrated, leading as a typical result of the automatic conclusion of the working chain operations. The utility of the maximum exposure time input value has been demonstrated. A comparison was made, on several trials, between the actual acquisition duration of a batch of five measurements and the theoretical value taken from the datasheet, noting an average percentage difference between these of about 1.95 %. The validation phase was also exploited to suggest to the user a recommended values range concerning the phase ON to be chosen as the GUI input parameter. This proposed range allows the user not to run into presumed situations of operational incompatibility between the software and piloted instrumentation and to exploit as much as possible the counter implemented via software relating to the maximum exposure time, thus increasing the possibilities for which the target temperature is considered reached ("Target reached" algorithm branch) to the ones that target temperature is considered exceeded ("Target exceeded" algorithm branch). The recommended range is thus between 5 and 20 s. The functionality of the IR irradiation pause button was also demonstrated, as well as the reaction of the system in case of target temperature lower than room temperature,

The tool developed in this thesis work thus provides self-adjusting temperature control of irradiated neural tissue samples. It will undoubtedly be necessary to evaluate the functionalities validated in this thesis work on real tissue samples, for example by comparing the actual cycle-by-cycle induced temperature jump with the theoretically stated one, or the reliability of the nature of the acceptance range chosen to contrast the uncertainty of measurements when evaluating calculated ΔT errors.

Among the possible uses for brain researchers during in vivo and in vitro tests, the CLC system could be used to evaluate hyperthermia phenomena in epileptic subjects or TBI or to simulate them (although only locally, since pathological hyperthermia is a more global, widespread phenomenon), to perform thermal stress tests of infrared neural stimulation (INS) or inhibition (INI) or to assess optimal output optical power values for possible therapeutic purposes.

8 Acknowledgement

First of all a heartfelt thanks to Ágoston Horváth and Zoltán Fekete, who with their excellent availability and their collaboration, have continuously helped me to complete, with great satisfaction, this master thesis work, despite the many difficulties that the current global pandemic has placed between us never giving me the chance to reach Budapest physically. We did it, though. Thank you. I hope to continue to make my small contribution to Hungarian neuroscientific research through this beautiful initiative, even after my graduation.

Thanks to the Research Group of Implantable Microsystems, Pázmány Péter Catholic University, and the Hungarian Academy of Sciences for the laboratory equipment and all the support material provided to me.

Grazie alla Professoressa Agostini, per il suo supporto durante la stesura.

Grazie a mamma, papà, Leo e Ciccio, la mia vera e unica Famiglia. Senza di voi, io non sarei qui a scrivere i ringraziamenti della mia tesi di laurea. Nonostante le intemperie che la vita ci ha posto davanti, le incertezze sul futuro, i mille “ma”, mi avete reso quel che sono. Non avrei potuto chiedere di meglio in nessun'altra vita.

Grazie a Noemi, il mio faro, il mio supporto costante (costante!), il mio mantra assoluto. La mia metà. Non basterà il tempo a me a disposizione per dimostrarti la mia graditudine nello starmi sempre vicino, nei momenti più e meno piacevoli. In queste pagine, ci sei anche tu.

Grazie a Pausamerda e CaWalter, gli amici che sai sceglierti e che non vorresti cambiare mai. Spero non passi molto tempo da questo momento, perché si possa tornare a rivivere la nostra quotidianità insieme.

Grazie ad Alessia, amica vera e storica. Abbiamo condiviso tante emozioni, estati in biblioteca a preparare esami diversi, gioie e dolori universitari e non. Non ci perderemo.

Grazie ad Andrea e Pasticcino, compagni di giochi e tante fesserie. Se quando torno a casa son felice è anche per merito vostro.

Grazie a Mimmo e Matti, amici preziosi prima che colleghi, con cui ho passato innumerevoli momenti (esami e progetti!) durante questi cinque anni insieme. Ho imparato molto da voi.

Grazie a Riccardo, un fratello mancato che conosco da una vita e con un destino comune. Spero di essere per te un esempio come tu lo sei per me.

Grazie a Federico Zinga, Adriano, Enio, Mr Carlo, le Papere Sara e Silvia, Giulia, Leti, Sara, Fabio, Daniele, Ruggero, Dassista, Lorenzo Addati e i miei amici dell'Erasmus.

9 References

- [1] K. L. S. Sharma, “Overview of Industrial Process Automation.” 2011.
- [2] S. Santaniello, G. Fiengo, L. Glielmo, and W. M. Grill, “Closed-Loop Control of Deep Brain Stimulation : A Simulation Study,” vol. 19, no. 1, pp. 15–24, 2011.
- [3] H. L. Wade, “Basic and Advanced Regulatory Control : System Design and Third Edition,” 2017.
- [4] E. M. Dunn and M. M. Lowery, “Simulation of PID Control Schemes for Closed-Loop Deep Brain Stimulation,” *2013 6th Int. IEEE/EMBS Conf. Neural Eng.*, pp. 1182–1185, 2013, doi: 10.1109/NER.2013.6696150.
- [5] E. A. Kiyatkin, “Brain temperature and its role in physiology and pathophysiology : Lessons from 20 years of thermorecording Lessons from 20 years of thermorecording,” *Temperature*, vol. 6, no. 4, pp. 271–333, 2019, doi: 10.1080/23328940.2019.1691896.
- [6] P. Koppa *et al.*, “Infrared neural stimulation and inhibition using an implantable silicon photonic microdevice,” 2020.
- [7] H. Wang *et al.*, “Brain temperature and its fundamental properties: A review for clinical neuroscientists,” *Front. Neurosci.*, vol. 8, no. SEP, pp. 1–17, 2014, doi: 10.3389/fnins.2014.00307.
- [8] A. Szallasi, *TRP Channels as Therapeutic Targets: From Basic Science to Clinical Use*. Academic Press, 2018.
- [9] J. A. Kauer and H. E. Gibson, “Hot flash: TRPV channels in the brain,” *Trends Neurosci.*, vol. 32, no. 4, pp. 215–224, 2009, doi: 10.1016/j.tins.2008.12.006.
- [10] M. Tominaga, “TRP Ion Channel Function in Sensory Transduction and Cellular Signaling Cascades.” 2007.
- [11] M. J. Caterina, M. A. Schumacher, M. Tominaga, T. A. Rosen, J. D. Levine, and D. Julius, “The capsaicin receptor: a heat-activated ion channel in the pain pathway,” *Nature*, vol. 389, no. 6653, pp. 816–824, 1997, doi: 10.1038/39807.

- [12] Z. Fekete and A. Zatoryi, “Infrared neuromodulation : a neuroengineering perspective,” no. September, 2020, doi: 10.1088/1741-2552/abb3b2.
- [13] M. A. Naeser, M. D. Ho, P. I. Martin, M. R. Hamblin, and B.-B. Koo, “Increased Functional Connectivity Within Intrinsic Neural Networks in Chronic Stroke Following Treatment with Red/Near-Infrared Transcranial Photobiomodulation: Case Series with Improved Naming in Aphasia.,” *Photobiomodulation, photomedicine, laser Surg.*, vol. 38, no. 2, pp. 115–131, Feb. 2020, doi: 10.1089/photob.2019.4630.
- [14] L. L. Chao, “Effects of Home Photobiomodulation Treatments on Cognitive and Behavioral Function, Cerebral Perfusion, and Resting-State Functional Connectivity in Patients with Dementia: A Pilot Trial.,” *Photobiomodulation, photomedicine, laser Surg.*, vol. 37, no. 3, pp. 133–141, Mar. 2019, doi: 10.1089/photob.2018.4555.
- [15] A. Mahadevan-Jansen, K. Mariappan, J. Albea, P. E. Konrad, and E. D. Jansen, “Optical stimulation of neural tissue,” *Conf. Proc. - Lasers Electro-Optics Soc. Annu. Meet.*, vol. 1, no. 5, p. 372, 2003, doi: 10.1109/leos.2003.1251809.
- [16] A. D. Izzo *et al.*, “Laser stimulation of auditory neurons: Effect of shorter pulse duration and penetration depth,” *Biophys. J.*, vol. 94, no. 8, pp. 3159–3166, 2008, doi: 10.1529/biophysj.107.117150.
- [17] D. K. S. Nishijima David L; Wisner, David H; Holmes, James F, “Optical pacing of the embryonic heart,” *Physiol. Behav.*, vol. 176, pp. 139–148, 2016, doi: 10.1016/j.physbeh.2017.03.040.
- [18] Q. Liu, M. J. Frerck, H. A. Holman, E. M. Jorgensen, and R. D. Rabbitt, “Exciting cell membranes with a blustering heat shock,” *Biophys. J.*, vol. 106, no. 8, pp. 1570–1577, 2014, doi: 10.1016/j.bpj.2014.03.008.
- [19] H. T. Beier, G. P. Tolstykh, J. D. Musick, R. J. Thomas, and B. L. Ibey, “Plasma membrane nanoporation as a possible mechanism behind infrared excitation of cells,” *J. Neural Eng.*, vol. 11, no. 6, 2014, doi: 10.1088/1741-2560/11/6/066006.
- [20] M. Ganguly, M. W. Jenkins, E. D. Jansen, and H. J. Chiel, “Thermal block of action potentials is primarily due to voltage-dependent potassium currents: A modeling study,” *J. Neural Eng.*, vol. 16, no. 3, 2019, doi: 10.1088/1741-2552/ab131b.

- [21] Á. C. Horváth, Ö. C. Boros, S. Beleznai, Ö. Sepsi, P. Koppa, and Z. Fekete, “A multimodal microtool for spatially controlled infrared neural stimulation in the deep brain tissue.”
- [22] T. V. F. Abaya *et al.*, “Characterization of a 3D optrode array for infrared neural stimulation,” *Biomed. Opt. Express*, vol. 3, no. 9, p. 2200, 2012, doi: 10.1364/boe.3.002200.
- [23] V. B. Brooks, “Study of brain function by local, reversible cooling. In: Reviews of Physiology, Biochemistry and Pharmacology,” in *Reviews of Physiology, Biochemistry and Pharmacology*, H. Springer, Berlin, Ed. 1983, p. Vol. 95, pp 1–109.
- [24] Keithley Instruments, “Series 2600B System SourceMeter ® Instrument Reference Manual,” no. August, 2016.
- [25] Keithley Instruments, “6½-Digit USB Digital Multimeter 6½-Digit USB Digital Multimeter.”